Naval Research Laboratory

Washington, DC 20375-5320

NRL/MR/5603--96-7886

Fiber Optic Infrared Cone Penetrometer: Results of the May 1995 Field Test

F. BUCHOLTZ
I. D. AGGARWAL
S. T. VOHRA
K. J. EWING

Fiber Optic Environmental Sensors Section
Optical SciencesDivision

G. M. NAU

University Research Foundation

J. A. MCVICKER

SFA, Inc.
Landover, MD

November 26, 1996

DISCLAIMER NOTICE

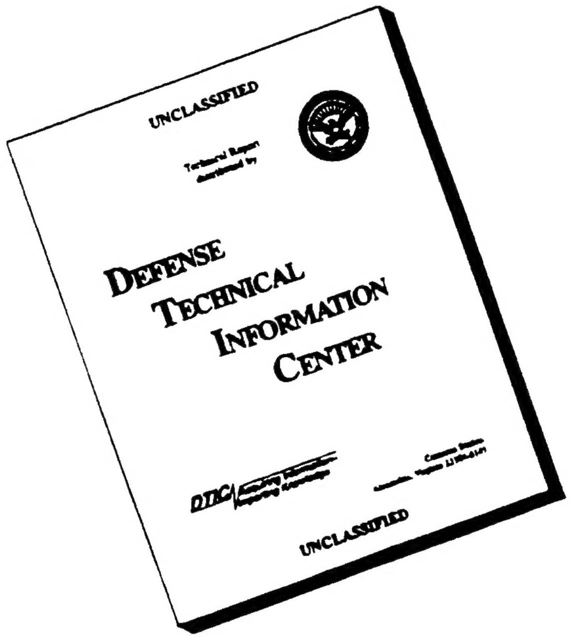

THIS DOCUMENT IS BEST QUALITY AVAILABLE. THE COPY FURNISHED TO DTIC CONTAINED A SIGNIFICANT NUMBER OF PAGES WHICH DO NOT REPRODUCE LEGIBLY.

REPORT DOCUMENTATION PAGE

Form Approved
OMB No. 0704-0188

1. AGENCY USE ONLY *(Leave Blank)*	2. REPORT DATE	3. REPORT TYPE AND DATES COVERED
	November 26, 1996	

4. TITLE AND SUBTITLE

Fiber Optic Infrared Cone Penetrometer: Results of the May 1995 Field Test

5. FUNDING NUMBERS

6. AUTHOR(S)

Frank Bucholtz, Gregory M. Nau,* Ishwar D. Aggarwal, Sandeep T. Vohra,
Kenneth J. Ewing, and James A. McVicker**

7. PERFORMING ORGANIZATION NAME(S) AND ADDRESS(ES)

Naval Research Laboratory
Washington, DC 20375-5320

8. PERFORMING ORGANIZATION REPORT NUMBER

NRL/MR/5603--96-7886

9. SPONSORING/MONITORING AGENCY NAME(S) AND ADDRESS(ES)

U.S. Army Environmental Center
SFIM-AEC-ETP
Aberdeen Proving Ground, MD 21010-5401

10. SPONSORING/MONITORING AGENCY REPORT NUMBER

11. SUPPLEMENTARY NOTES

*University Research Foundation
**SFA, Inc., Landover MD

12a. DISTRIBUTION/AVAILABILITY STATEMENT

Approved for public release; distribution unlimited.

12b. DISTRIBUTION CODE

13. ABSTRACT *(Maximum 200 words)*

A fiber optic system for remote, in-situ detection of hydrocarbon contimination in soils was developed for use with the cone penetrometer. The system uses infrared transmitting chalcogenide fibers to measure the infrared spectrum of light diffusely reflected from the soil undergound to identify and quantify organic contiminants such a fuels, oils, chlorinated compounds, and BTEX compounds (benzene, toluene, ethylbenzene, and xylene). A field test of the prototype system was conducted at Dover AFB in May 1995. The results of the test are summarized in this report. A system of this type is important for rapid, cost-effective site characterization and environmental cleanup.

14. SUBJECT TERMS

Chemical sensors	Fiber optic sensors
Environmental sensors	Cone penetrometer
Polycyclicaromatic hydrocarbon	

15. NUMBER OF PAGES

61

16. PRICE CODE

17. SECURITY CLASSIFICATION OF REPORT	18. SECURITY CLASSIFICATION OF THIS PAGE	19. SECURITY CLASSIFICATION OF ABSTRACT	20. LIMITATION OF ABSTRACT
UNCLASSIFIED	UNCLASSIFIED	UNCLASSIFIED	UL

CONTENTS

FIBER OPTIC INFRARED CONE PENETROMETER: RESULTS OF THE MAY 1995 FIELD TEST

1. Executive Summary

• Data from the first field test of the fiber optic cone penetrometer system conducted at Dover AFB was compiled and analyzed and an assessment was made of overall system hardware performance.

• The value of adopting a modular design for the fiber optic IR system was proven after one tube was bent during operation without affecting the operation of the IR system. The optical system was simply removed from the bent tube and inserted in a new tube (Fig. 3).

• The test demonstrated that cabled chalcogenide fibers can be handled without special precautions in the SCAPS environment and that they are rugged enough for general use in the field (Fig. 11).

• Low optical signal levels showed that efficiency of the optical system was the single most important system improvement to be made before the next test (Fig. 12).

• Low TCE levels in the soil coupled with low optical signal levels prevented detection of chlorinated hydrocarbons in the field during this first field test (Figs. 25 & 26). However, the survivability, ruggedness, and ease of use of the hardware system was successfully demonstrated.

• Work is currently in progress to improve the efficiency of the optics that collect light diffusely-reflected from the soil with a goal of approximately a factor of 10-20 times increase.

• Calculations show that this type of system should ultimately provide detection limits in the range 0.5 - 10 ppm depending on type of contamination, type of soil, and soil moisture conditions (Figs 27 & 28).

Manuscript approved July 18, 1996.

2. FIELD TEST

2.1 Background

The first field test of the NRL fiber optic infrared cone penetrometer system was conducted May 8-11, 1995 at Dover AFB. Tests of the fiber optic infrared system were part of larger suite of tests performed using the SCAPS truck under the direction of Dr. William Davis, US Army Waterways Experiment Station. The purposes of the infrared fiber optic test were: i) to demonstrate the ability of a chalcogenide-based fiber cable and infrared spectrometer to work successfully in the field in the SCAPS system, and ii) to detect and quantify hydrocarbon contaminants in the soil, especially chlorinated solvents such as TCE.

2.2 Sysytem Hardware

A block diagram of the system is shown in Fig. 1. The penetrometer tube contains a source of IR radiation (nichrome wire) operating at approximately 1000K equivalent blackbody temperature, a pair of paraboloidal mirrors to direct light out through a sapphire window into the soil and to collect diffusely-reflected light, and a focusing lens to inject the collected light into the IR-transmitting chalcogenide fiber. The cabled fiber transmits light to the FTIR spectrometer and the resulting infrared spectrum contains information on the type and quantity of chemical contaminants in the soil. This system is most sensitive to liquid contaminants in the soil such as dense non aqueous phase liquids (DNAPLs) and non aqueous phase liquids (NAPLs) and has the advantage of the ability to detect chlorinated hydrocarbon solvents.

The enabling technology for this system is the infrared-transmitting optical fiber. This fiber, developed and fabricated at NRL, is based on chalcogenide materials (As_2S_3, As_2Se_3, or As_2Te_3) and transmits light in the wavelength range 2 - 12 μm and thus can be used to perform remote, in-situ IR spectroscopy. The properties of the three cables fabricated for the field test were summarized in a previous report and are repeated here in Table 1. Figure 2 is a photograph of the endface of the 3F10M cable showing the arrangement and size of the fibers.

Table 1. Properties of chalcogenide fiber cables fabricated for May 95 field test.

Cable	Number Fibers	Length(m)	Fiber Diam (μm)	Total Fiber Endface Area (μm^2)	Min Loss (dB/m)	Loss @ λ=3.4 μm (dB/m)
1F12M	1	12	200	3.1×10^4	0.20	0.22
1F20M	1	20	250	4.9×10^4	0.25	0.25
3F10M	3	10	250	14.7×10^4	0.25	0.27

For these cables, all fibers are Teflon-clad, core-only As_2S_3.

The mechanical design of the penetrometer tube used for the fiber optic IR system was nearly identical to the one used for the SCAPS laser-induced fluorescence (LIF) system. One exception was the sapphire window holder which was modified slightly for our system to allow greater optical throughput.

A completely new insert to the tube for the infrared optical system was designed and fabricated. To facilitate benchtop alignment and repair in the field, if necessary, the IR optical components in the penetrometer tube (source, collimating lens, paraboloidal mirrors, focusing lens, and cable strain relief) were attached to a "rail" which slides in and out of the penetrometer tube and which is attached to the tube by screws from the underside. Figure 3 is a photograph of the rail assembly.

Three complete rail assemblies were fabricated and tested at NRL prior to testing. Two complete penetrometer tubes were fabricated by WES for use in the test. Hence, two complete penetrometer tube systems were available for the field test, each containing a rail, one attached to cable 1F20M and one attached to cable 3F10M (Table 1) as shown in Fig. 4 . The two systems are shown in their shipping case in Fig. 5.

A complete set of mechanical drawings for the rail, optical components, modified sapphire window, and cable seal is available [G. N. Nau (202-767-9505), "IR Reflectance Probe for the Cone Penetrometer SCAPS System - Mechanical Drawings"]

The FTIR spectrometer system used was a KVB/Analect FX 70 with KBr optics operated in bistatic mode (remote IR source). The principal instrumentation components of the system are shown in Fig. 6. A short rack (Fig. 7) containing the IR source power

supply (Kepco BOP 36-6M), the FTIR electronic signal processor (KVB/Analect DCM-30), and the FTIR optical interferometer (KVB/Analect TSO-40) was positioned in the SCAPS truck near the push hydraulics. A 4 mm diameter, liquid-nitrogen-cooled InSb photodetector with 5.5 μm cut-off wavelength was used. During operation, the interferometer box was continually purged with dry nitrogen. The PC computer for system operation and data acquisition was located in the "clean" room in the SCAPS truck. Figure 8 shows the display screen of the computer during operation, in this case, in the laboratory using a sample cell designed to fit in the sapphire window opening in the tube. These cells allow samples of various soil and contaminant types to be tested. The cell shown in Fig. 8 contains sand with diesel fuel (DFM) contamination and the IR absorption signature of a diesel fuel is evident in the spectrum shown on the screen.

2.3 Description of Field Test

Upon arrival at the test site on the morning of Monday, May 8 the NRL system was unloaded, assembled and operational within approximately 1.5 hrs. The fiber optic cable was first connected to the FTIR to check system operation and then disconnected temporarily to allow the cable to be threaded through additional push tubes. Figure 9 shows the chalcogenide fiber cable "strung through" a number of push tubes on the rack in the SCAPS truck.

A map showing the location of push holes near Bldg 719 at Dover AFB is shown in Fig. 10. In addition to the pushes near Bldg 719, pushes were made using the fiber optic IR system at two locations: i) a grassy area on the north-south runway of Dover AFB, and ii) near the 10th tee of the Dover AFB golf course. Table 2 summarizes the push locations for the fiber optic IR penetrometer tests. In total, 165 measurements were made in six different push holes over the 3 1/2 day test period. The file names and test conditions for each measurement are tabulated in Appendix A. The following general methodology was followed for each push:

1) The penetrometer tube was placed horizontal on the floor of the SCAPS truck and a diffuse gold reflector ("gold reference") was placed on the sapphire window. The x-y-z position of the cable input to the FTIR was manually adjusted to maximize the optical signal received by the FTIR as determined by the "A/D %" value shown on the FTIR display.

Table 2. Push locations for the fiber optic IR cone penetrometer system during the May 1995 field test at Dover AFB. See map in Fig. 10 for geographical locations near Bldg. 719.

NRL Hole Designation	WES Hole Designation	Comment
9	9	Near Bldg 719
10	10	Near Bldg 719
POL	11	Site on runway grassy area expected to contain JP fuel spill
GC-1	12	Site on golf course (10th tee) expected to contain oil
GC-2	13	Site on golf course (10th tee) expected to contain oil
14	14	Near Bldg 719 near sewer tube

2) The tube was then inserted into the hydraulic assembly and pushed into the ground. The penetrometer was stopped at various depths while the IR spectra were recorded. Typically, 200 scans were recorded at a given depth requiring approximately 200 seconds total at each depth.

3) After the penetrometer was brought back up out of the ground the optical signal level was again recorded with the gold reflector in place.

4) Typically, two additional measurements were made after the tube had been brought up. IR spectra were recorded i) with the gold reference removed; and ii) with the fiber cable disconnected from the FTIR input. These two measurements provided a measure of the background signal, that is, the optical signal containing no information from the soil but due to stray light and room temperature blackbody radiation.

2.4 Discussion of Results

A critical goal of this test was the demonstration of the survivability and ruggedness of the cabled chalcogenide fiber. Prior to the test, chalcogenide fiber had been cabled in lengths of approximately one meter. For this test, fibers in lengths ranging from 10 to 50 meters were fabricated and tested at NRL and were cabled in shorter lengths by Foster-Miller, Inc. A summary of the properties of the three cables, as presented in the last report, was given above in Table 1. For all measurements taken after the morning of May 8, the 3-fiber bundle cable 3F10M was used since this cable exhibited the highest optical throughput. A comparison of the performance of the cable in the field to the performance

in the laboratory could be made by comparing the raw optical power spectra with the gold reflector on the penetrometer window (Step #1 of the test methodology described above). The results are shown in Fig. 11 for one measurement taken in the laboratory just before the field test and one measurement taken in the field (Filename DOV093) taken on May 9 after the system had been in operation for approximately 1 1/2 days and the cable had been handled repeatedly by the SCAPS truck operators. Fig. 11 shows virtually no difference between the optical throughput of the cable in the laboratory and in the field. Small differences in the spectrum are attributable to small differences in the temperature of the thermal source in the penetrometer. **This result demonstrates that cabled chalcogenide fibers can be handled without special precautions in the SCAPS environment and that they are rugged enough for general use in the field.** In effect , cabled chalcogenide fibers are just as robust as currently-used silica fibers for field use.

During the push at Hole 11 on Tuesday, May 9, a hardpan layer was encountered just below the surface and hydraulic force near the limit available was required to push the penetrometer through. After completing this push, it was discovered that the penetrometer tube had bent during the hard push. The deformation, amounting to approximately 0.1 inch over the length of the tube, had no adverse effect on the operation of the IR optical system in the tube. On Tuesday evening, the optical rail and cable were removed from this tube and inserted in the remaining good tube for the remainder of the tests. **This incident proved the value of adopting a modular design for the fiber optic IR system and proved the robustness of the cone portion of the optical system.**

Soil in the Dover AFB area ranges from sand to silt to clay. In most cases, a significant amount of water is present and the water table easily extends up to within approximately 10 feet of the surface. A quick examination of the data (See Appendix A) reveals that the optical power recovered from the system when it was in the soil was not significantly different from the power when the tube was out in the air. For example, from the data for 9 May 95 (Hole 11), the optical power with the probe out of the ground and with nothing on the window was A/D % = 42 [Run (Filename) DOV095]. With the probe in the ground, the A/D% varied from 59 to 39. Hence, at best, the total optical power received from the soil was 50% larger then the background power level and, at worst, there was no measurable optical power from the soil. (The A/D value is proportional to the total optical power which, for low signal powers, can be dominated by ambient room

temperature thermal radiation.) The situation is summarized in Fig. 12 which compares the raw (un-normalized) optical power spectra for four cases: i) with the gold reference reflector positioned on the penetrometer window (corresponding to the maximum possible optical throughput of the system); ii) in the laboratory with dry sand in a sample cell ; iii) in-ground at Dover AFB (Filename DOV063); and iv) with the cable disconnected corresponding to the ambient background spectrum. This figure clearly shows that the margin between the background level and the signal level (Case iii), for what is presumably water-saturated clay soil, is small in the region above 3 μm and that, under these conditions, the signal-to-noise ratio will be substantially lower than in the case of dry sand (Case ii). The large relative power due to background radiation has the effect of reducing the apparent depth of absorption bands due to hydrocarbons in the soil.

This effect can be quantified as follows. Let the band depth be given by $\Delta P/P_o$ as shown in Fig. 13. In this ideal case, $\Delta P/P_o = (P_o-P_\sigma) / P_o$ where information on the type and quantity of chemical contamination is contained in the position and strength of the "signal" power P_σ. However, if background power P_b is present in addition to the signal power, then the observed band depth is

$$(\Delta P/P_o)_{obs} = (P_o-P_\sigma) / (P_o+P_b) = K(\Delta P/P_o)$$

where $K = 1/(1+P_b/P_o)$. In the limit $P_b >> P_o$, the observed band depth becomes vanishingly small. Hence, the results of Fig. 12 indicated that the optical efficiency of the current system, although satisfactory for dry, sandy soil, would need to be improved significantly in order to provide useful information in wet soil. **Work is currently in progress to improve the efficiency of the optics that collect light diffusely-reflected from the soil with a goal of approximately a factor of 10-20 times increase.**

Spectra taken at various depths in Holes 10,11,12 and 14 are shown in Figs. 14 - 17 for the C-H stretch region of the mid-infrared 3.2 - 3.8 μm. Arbitrary offsets have been added to visually separate the traces and comparison of the absolute power levels can be obtained from the A/D values in Appendix A. These spectra have not been normalized to the instrument transfer function (gold reference).

As discussed above in connection with Fig. 12, the spectra at wavelengths greater than approximately 4 μm is dominated by background (room temperature) blackbody

radiation. The data for Holes 11 and 13 show IR absorption features near 3.4 μm and 3.5 μm, indicative of the presence of hydrocarbons. However, after normalizing the spectra to the instrument transfer function the features disappear[1]. (HC features are not apparent in the data from Holes 10 & 12 due to low optical power levels.) Hence, unfortunately, these hydrocarbons are present in the instrument itself, mainly in coatings in the spectrometer windows , on the mirrors and beam splitter of the interferometer, and in the fiber itself. This effect is well known in the FTIR community and has been observed by other workers. Although the coatings are typically inorganic dielectric materials, hydrocarbon contamination inevitably occurs in the batch materials and in the vacuum pumping system used in the formation of the coatings. Quite simply, the world is rich in manmade hydrocarbons and complete removal of all contamination in any IR spectrometer system would be an expensive undertaking. Contamination is an especially serious problem when it is present in the beam splitter or on the mirrors since the contaminant layer then exists in one arm of the interferometer where small amounts of hydrocarbon can give rise to much larger variations inside the interferometer output than the same amount of hydrocarbon outside the interferometer. We are currently discussing the problem with spectrometer manufacturers but , at this point, it is unlikely that significant improvements will be made in the near future. Since the absorption feature due to instrument contamination is relatively constant in time, it effectively becomes part of the instrument response function and can be eliminated, in principle, by the standard technique of normalizing the data spectrum by the instrument response function. However, difficulties arise when the optical power level from the sample is low and when measurable temporal variations occur in the response function.

Data from Hole 14 (Fig. 17), taken on the last morning of the test shows extremely poor signal to noise ratio. After returning to NRL, it was discovered that the KBr optics in the FTIR interferometer had been severely damaged by moisture. KBr is hygroscopic and prior to the test we understood the risks in taking this particular system into the field. The risk of moisture damage was increased by a particular mechanical design feature of this FTIR. The Analect spectrometer employs a Transept design in which the variable optical path difference is produced by a sliding wedge. Unless manually secured inside the interferometer box, the wedge can move during transport of the device and damage the drive mechanism. Hence, each time the SCAPS truck was moved, it was necessary to open the interferometer box which exposed the KBr optics to the atmosphere. We suspect

[1]The transfer function was calculated as the mean of the spectrum with the gold reflector in place and the spectrum with the cable disconnected.

the most serious damage occurred on May 10 and 11, both of which were rainy, humid days. However, the system continued to perform properly but at reduced performance level. This susceptibility to humidity will be eliminated for the second generation system by i) replacing the KBr optics with moisture-resistant CaF_2 optics, and ii) incorporating a mechanical system for securing the Transept wedge without opening the interferometer box.

In September 1995, laboratory analyses of soil samples taken near Holes 9 and 10 were completed by WES. Samples were analyzed for VOC's by EPA method 8260. The results (Courtesy of Dr. W. Davis, WES) are summarized in Appendix B. It is seen that for Hole 20, located between Holes 9 and 10, the TCE level was below 5 ppm (weight) at depths above 5 ft and rises to 290 ppm at 7 ft depth. (Presumably, 5 ppm represents the detection limit of the analytical technique.) These concentration levels are below the detection limit for the operation of the current fiber optic system under ideal conditions in the laboratory and detection under the low optical power levels in the field, as discussed above, was not possible. In addition, BTEX levels were also typically less than 5 ppm although at some depths the levels were on the order of tens of ppm. Once again, these levels are near the laboratory detection limits for dry sand and detection under the conditions encountered at Dover AFB was not possible.

Although actual TCE levels in the soil were too low to demonstrate detection of chlorinated hydrocarbons in the field during this first field test, the survivability, ruggedness, and ease of use of the hardware system was successfully demonstrated. Low optical signal levels showed that efficiency of the optical system was the single most important system improvement to be made before the next test.

In spite of the limitations discussed above, it was possible to perform remote spectroscopy in wet clay soil with the current system in the wavelength region below 2.3 μm where background thermal radiation is insignificant. Fig. 18 shows the absorption doublet due to kaolinite, a mineral component of clay soils, obtained from the IR spectra taken in Hole 10 (Fig. 14) near 5 ft depth. Fig. 19 shows the unnormalized spectra at various depths in the wavelength region 2.1-2.3 μm for the same Hole 10. The band depth of the kaolinite feature shows a smooth variation with soil depth as shown in Fig. 20. Although no independent chemical analysis was performed to determine kaolinite content, this behavior seems reasonable. The unnormalized spectra in the kaolinite region

for Holes 11,13, and 14 are shown in Figs. 21, 22, and 23, respectively. The strength of the kaolinite feature varies considerably from hole to hole and as a function of depth for a given hole, presumably reflecting variations in the kaolinite content. It would thus appear that the kaolinite content in the soil adjacent to Bldg. 719 (Holes 10 and 14) is measurably larger than the content at the golf course (Hole 13) or near the taxiway (Hole 11). It is worth noting that the kaolinite band is observable in the data from Hole 14 where the mid-IR (3.2-3.8 μm) data was extremely poor (cf. Fig. 17). Figure 24 shows a standard SCAPS CPT soil classification data set including LIF results for a push performed in the same Hole 12 on the golf course as measured with IR system. The data show the soil to be mainly silt and sand mixtures between depths 1.5 - 6 ft and mainly clay above and below. It would be instructive to compare CPT data from pushes near Bldg. 719, if available, to seek correlation with the IR data which showed higher kaolinite content near Bldg. 719 than on the golf course.

Soil samples were extracted from a push on the golf course near Holes 12 & 13 and sent to an independent laboratory (Gascoyne Laboratories, Inc.) for hydrocarbon analysis. Results of the analysis, performed for diesel fuel oil defined as C_{10} to C_{23} hydrocarbons, are presented in Appendix C. [Note: Samples A, B, and C listed on pg. App. C.3 were part of a laboratory study on sand soils and were <u>not</u> part of the field test.] This analysis did not include chlorinated hydrocarbons since the sample were not handled in a manner suitable which preserved volatile solvent content. The measured levels ranged from "not detectable" to a maximum 2400 ppm at 4 ft depth. In this case, we believe low optical signal levels in the wet clay soil prevented detection even at these levels.

In view of the important dependence of system performance on optical signal levels, it is worthwhile to calculate the expected performance of a system of this type. Ultimately, the performance depends on the ratio of signal power to noise on the photodetector. Noise on the photodetector is conveniently expressed by the so-called D* value from which the equivalent optical power noise of the detector can be determined. Photodetectors manufactured today typically exhibit D* values very close to the theoretical maximum limit due to fundamental fluctuations in the photon field. In this case, D* depends on only three parameters: detector cut-off wavelength λ_o, effective temperature of the signal source T_s, and the effective temperature of the background T_b. For an InSb detector with $\lambda_o = 5.5$ μm, $T_s = 1000$ K and $T_b = 293$ K, $D^* = 10^{11}$ $cm^{1/2} \bullet Hz^{1/2} / W$. The equivalent noise N is computed as $N = [A\Delta f]^{1/2} / D^*$ where A is the area of the photodetector and Δf is the electrical bandwidth. We have calculated the fundamental D*

detection limits for hydrocarbons on soil as a function of optical power P_o reaching the photodetector. Using the results of measurements of the dependence of absorption band depth on concentration for diesel fuel (DFM) and trichloroethylene (TCE) on sand and the D* value discussed above, the detection limits were calculated. Here we assumed the band depth was linearly related to weight fraction W of contaminant

$$\Delta P/P_O = \gamma W$$

where γ is approximately 10^{-4} ppm^{-1} for the C-H stretch absorption band in the mid-IR[2,3].

For the field test, the system was operated at 4 cm^{-1} resolution with an effective scanning speed of 1.44 cm/sec and used a 4 mm diameter InSb photodetector. With these parameters, the detection limit in ppm by weight[4] as a function of optical signal power level at the photodetector is presented in Figs. 25 and 26 assuming 100 scans per measurement and that the absorption line occurs near 3.3 µm (that is, in the mid-IR). γ is the slope of the calibration curve for band depth versus weight fraction defined above. Also shown are i) the approximate actual power levels which ranged from approximately 1 nW in dry sand to 0.1 nW in the clay soil at Dover AFB, and ii) the concentration levels given by the laboratory analysis of soil samples described above. These two parameters are combined to form a "box" as shown. The box in Fig. 25 is for the TCE levels determined from laboratory analysis (App. B) and the box in Fig. 26 is for heavy hydrocarbon levels (App. C). The optical power levels for dry sand were obtained in the laboratory and the level in the clay soil at Dover AFB was extrapolated using Fig. 12 as being a factor of 10 lower than in dry sand. Of course, even lower signal power levels are possible. The solid curve in these two figures corresponds to the detection limit. Hence, the intersection (if any) of the two shaded regions determines where detection is possible. It is seen in Fig. 25 that TCE levels were not high enough to be detected in wet clay. Detection of the heavy hydrocarbons encountered at Hole 12 would have been possible in dry sand but in wet clay, as shown, the available power is very near the detection limit. Note that the detection

---

[2] K.J. Ewing, T. Bilodeau, G. Nau, and I.D. Aggarwal, "Fiber optic infrared reflectance probe for detection of hydrocarbon fuels in soil," SPIE **2367**, 17-23 (1994).

[3] S.T. Vohra, F. Bucholtz, G.N. Nau, K.J. Ewing and I.D. Aggarwal, "Remote detection of trichloroethylene in soil by a fiber optic infrared reflectance probe," submitted to Applied Spectroscopy.

[4] Detection limit defined as three times the noise equivalent power (unity signal-to-noise ratio)

limit curve is not linear in this region of optical power levels due to the effect of thermal background power discussed above.

A set of similar curves for kaolinite will be useful but, at this time, we do not yet have the calibration curve for band depth versus kaolinite content.

It is important to understand the assumptions on which the first-order calculation leading to the detection limit figures was based[5]. 1) The absorption occurs at approximately 3.3 μm (3000 cm^{-1}). Since the D* value depends on wavelength, the detection limit curves will change as the observation wavelength changes even for the same photodetector and background temperature. 2) The calculation is based on the strength of the absorption band depth only - spectral curve fitting routines and spectral signal processing were not considered. 3) The calibration curve slope γ was obtained for sand samples and the effect of clay and water was assumed to be only a reduction in optical power level. Soil matrix effects such as chemical interactions, chemisorption, and physical absorption were not considered. More refined calculations of system performance will need to include these effects as they become better understood.

Using the same calculation, we can predict the improvement in detection limit expected with the improved optical system and using a photodetector with smaller area.

Figures 27 and 28 give the minimum detectable weight fraction (ppm) for 100 scans of the FTIR as a function of optical power on the photodetector at 3.3 μm wavelength for a 1x1 mm^2 InSb detector and 4 cm^{-1} resolution with approximately x20 improvement in optical throughput. For comparison purposes, we used the same TCE and heavy hydrocarbon levels as seen in the field test. **Hence, this type of system will ultimately provide detection limits in the range 0.5 - 10 ppm depending on type of contamination, type of soil, and soil moisture conditions.** As such, the additional capability to uniquely identify particular contaminants suggests that this system will provide an important tool for site characterization.

---

[5] F. Bucholtz, G.N. Nau, G. Hazel, K.J. Ewing, and I.D. Aggarwal, "Threshold detection limits for remote, fiber optic, FTIR spectroscopic sensors," submitted to Applied Optics.

3.Summary

Data from the first field test of the fiber optic cone penetrometer system conducted at Dover AFB was compiled and analyzed and an assessment was made of overall system hardware performance. The system hardware proved to be robust and easy to use with no hardware or software failures thus demonstrating that cabled chalcogenide fibers and FTIR spectrometry are suitable for use in the field and in the SCAPS system. Due to 1) low contaminant concentration, and 2) low reflected light levels no signals due to chlorinated hydrocarbons or fuels and oils were observed. Although we were not able to demonstrate detection of hydrocarbons in the field during this first field test, the survivability, ruggedness, and ease of use of the hardware system was successfully demonstrated. Low optical signal levels showed that improving the efficiency of the optical system was the single most important improvement to be made before the next test. In spite of the limitations discussed above, it was possible to perform remote spectroscopy in wet clay soil with the current system in the wavelength region below 2.3 μm where background thermal radiation is insignificant.

We have also made calculations of the best possible performance of a system of this type assuming fundamental photon fluctuation mechanisms as the limiting noise mechanism. The results suggest that, ultimately, this type of system should demonstrate detection limits in the range 0.5 - 10 ppm for a wide variety of hydrocarbon contaminants on soils ranging from dry sand to wet clay.

4. FIGURES

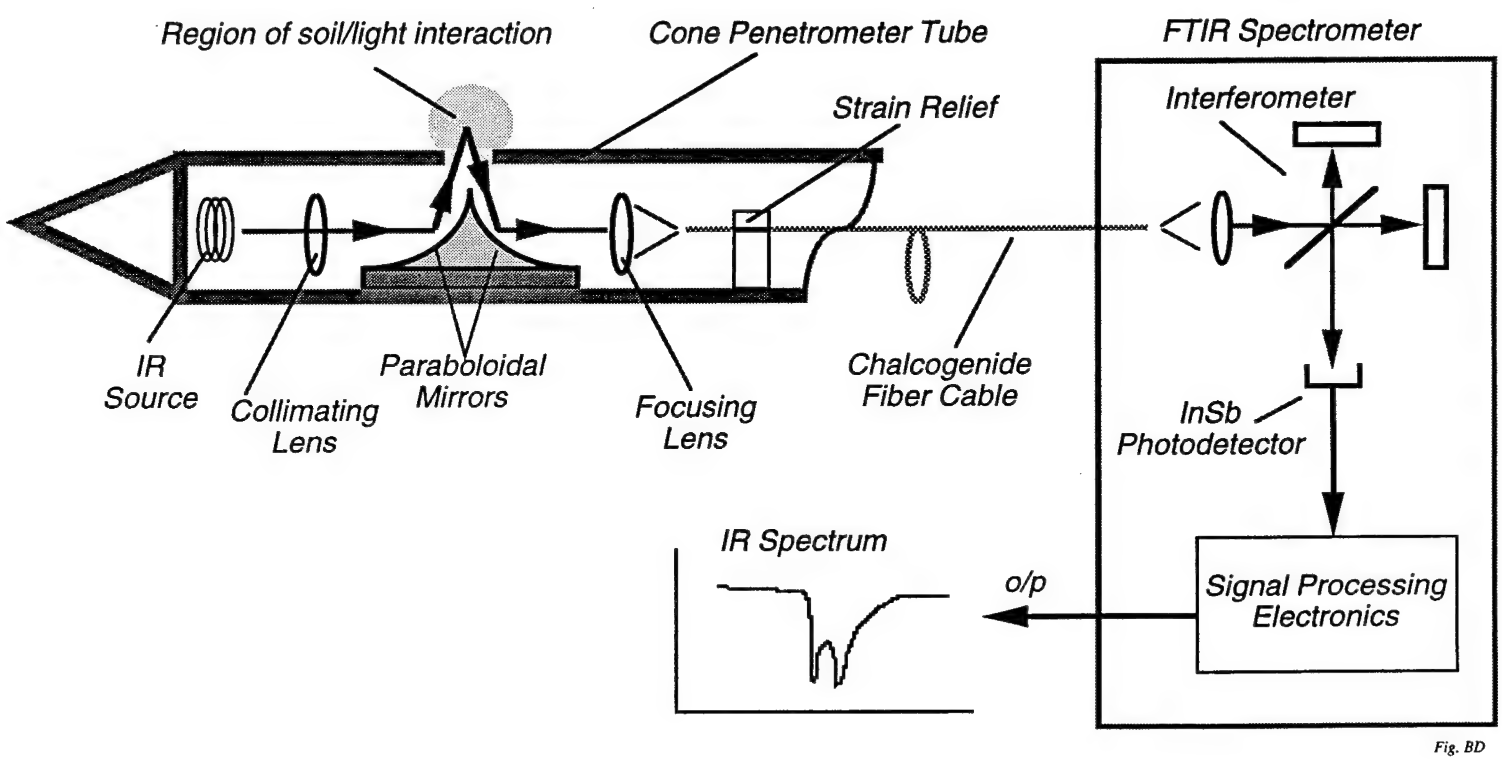

Fig. 1. Schematic diagram of the fiber optic IR cone pentrometer system. Dual parabaloidal mirrors direct light from the source to the soil and recovers diffusely-reflected light. The output of the Fourier Transform IR (FTIR) spectrometer is the IR spectrum characteristic of particular chemical contaminants in the soil.

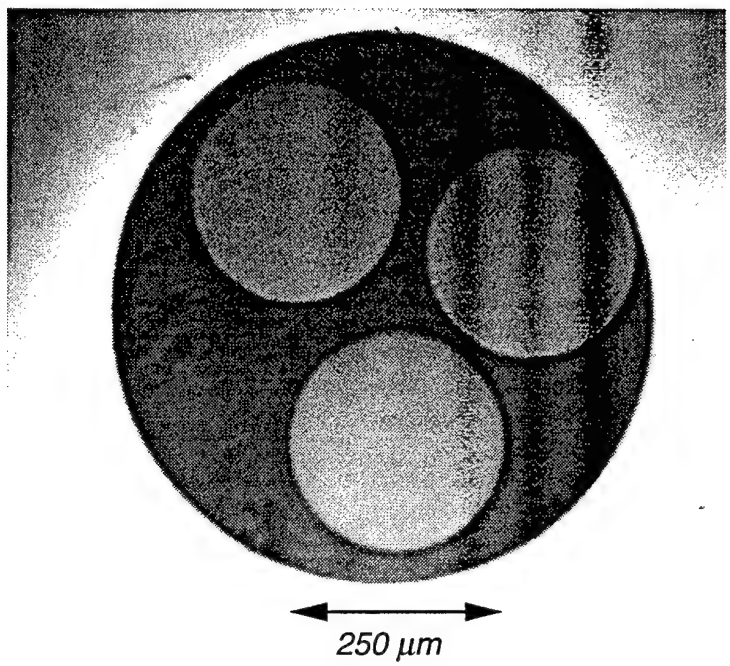

3-BUND-1.pict

Fig. 2. *Photograph of the endface of the 3-fiber cable 3F10M showing the three infrared-transmitting chalcogenide fibers.*

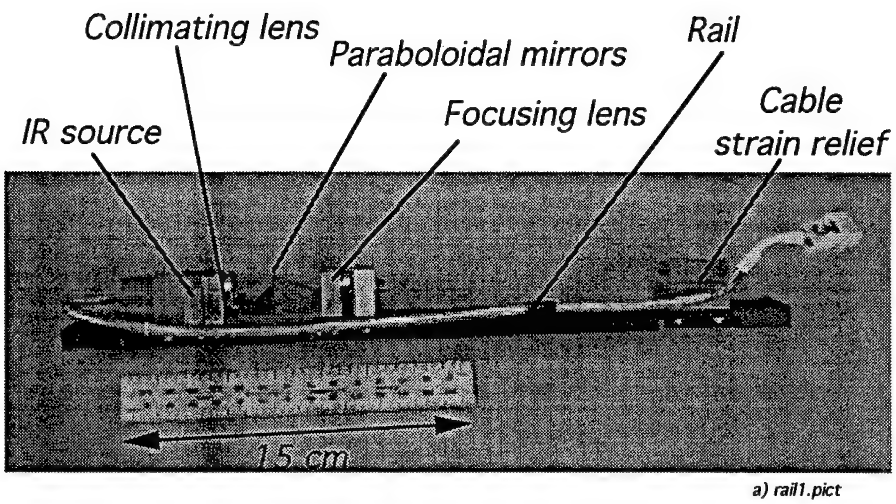

Fig. 3. Photograph of the rail assembly (cf. Fig. 1)

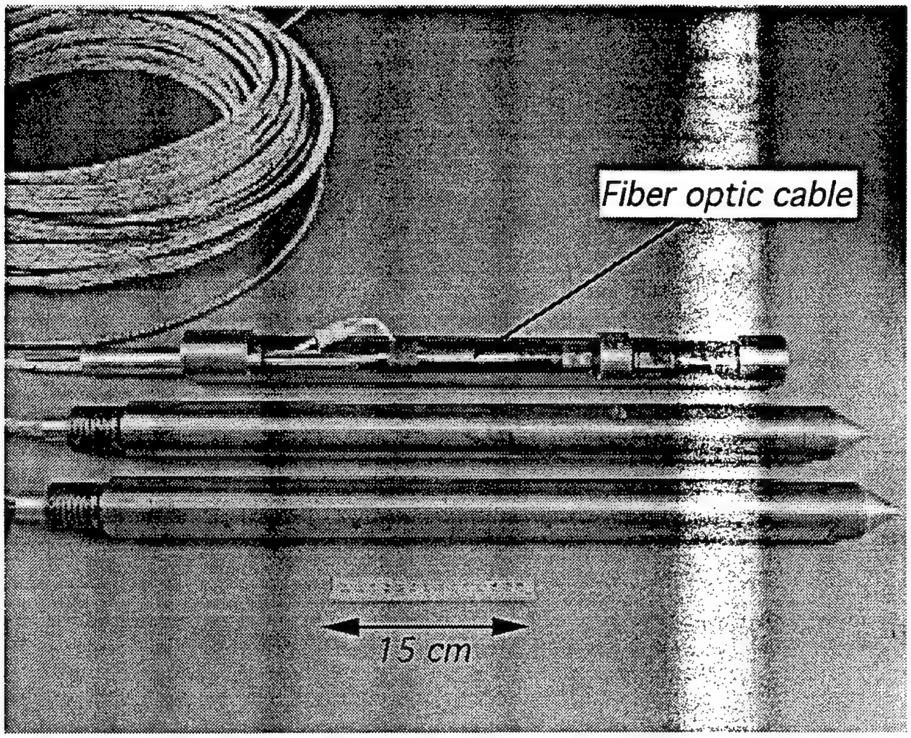

f) production.pict

Fig. 4. Photograph of cut-away tube for laboratory work (top) and two complete penetrometer tubes with cables attached.

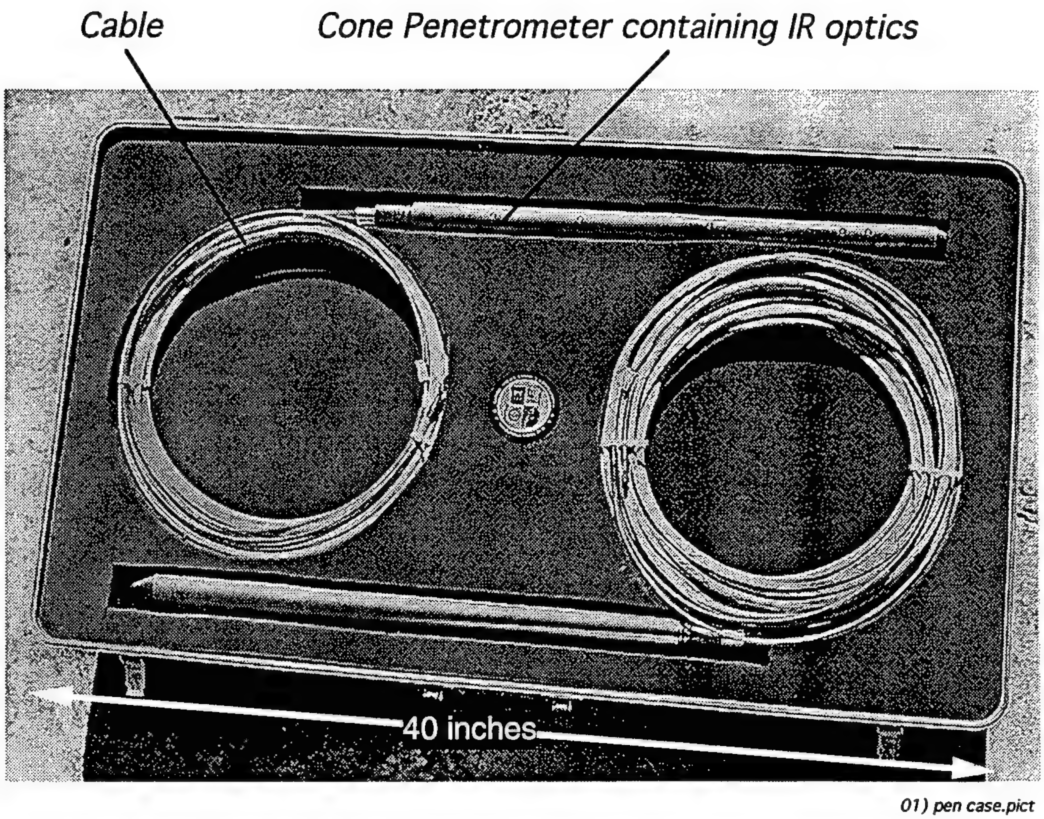

Fig. 5. Two complete fiber optic infrared cone penetrometers with attached cable containing chalcogenide fibers and electrical wires.

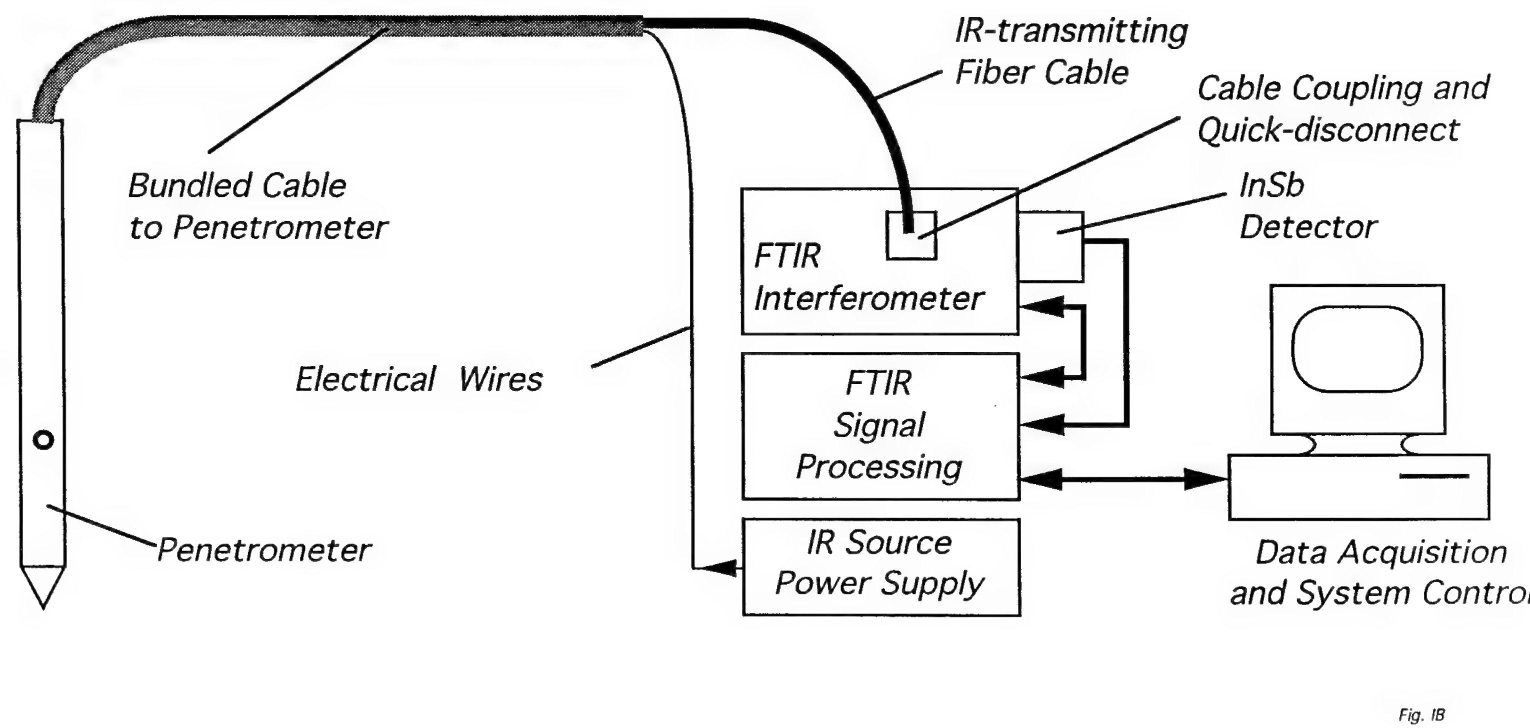

Fig. 6. *Block diagram of instrumentation*

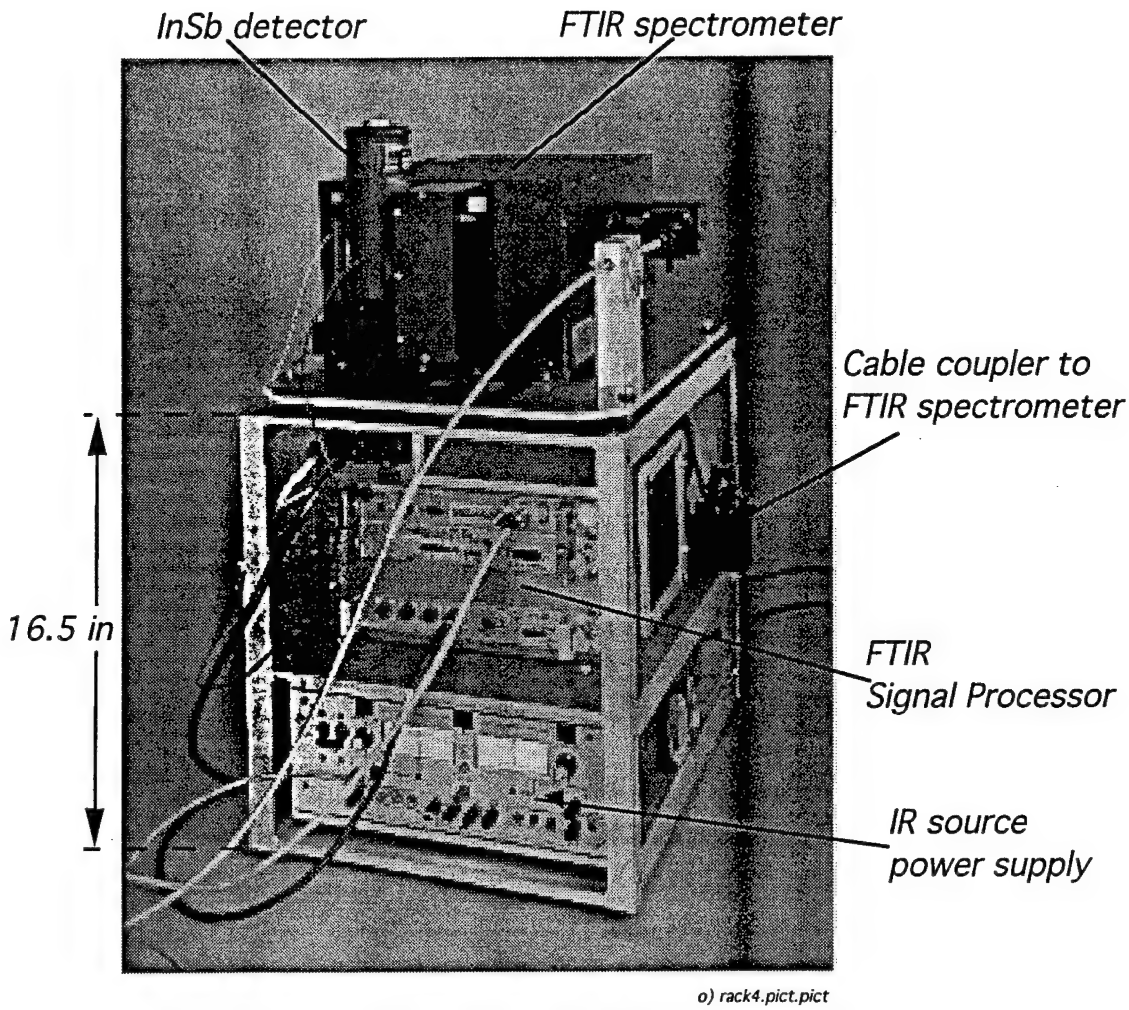

Fig. 7. Rack assembly showing the instrumentation components illustrated in Fig. 6.

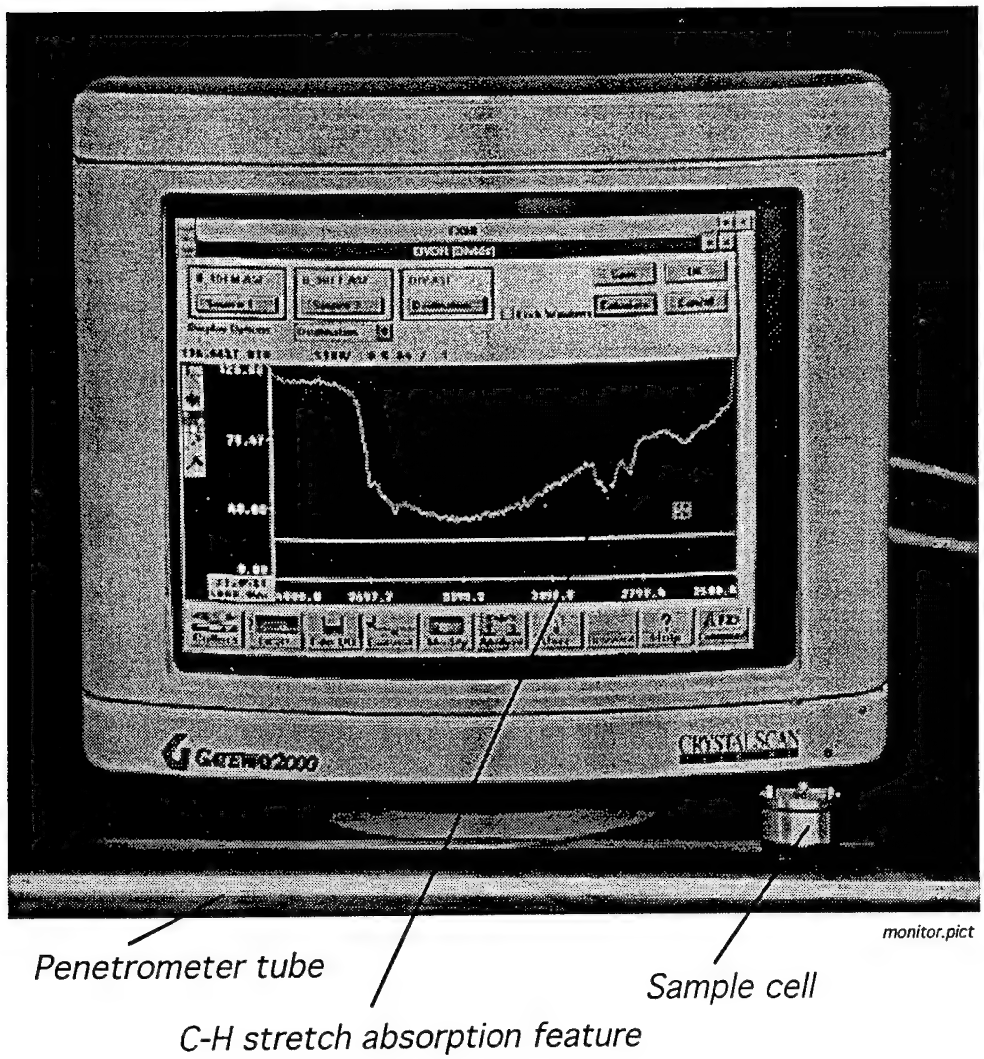

Fig. 8. IR spectrometer display panel. Spectrum shown was obtained with a sample cell containing a soil-hydrocarbon(DFM) mixture attached to the penetrometer tube.

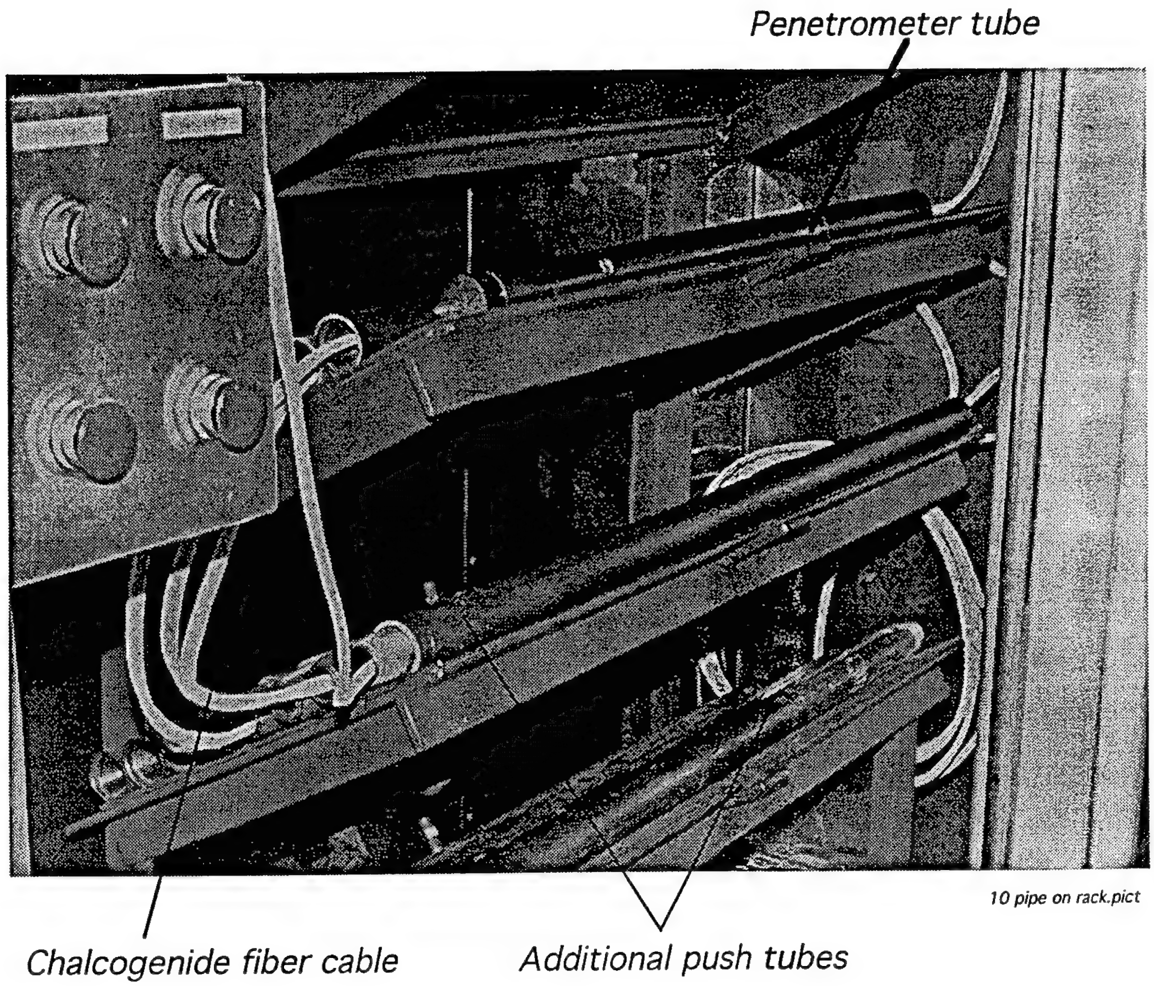

Fig. 9. The fiber optic infrared penetrometer on the rack in the SCAPS truck just prior to a push. The cable has been threaded through additional push tubes.

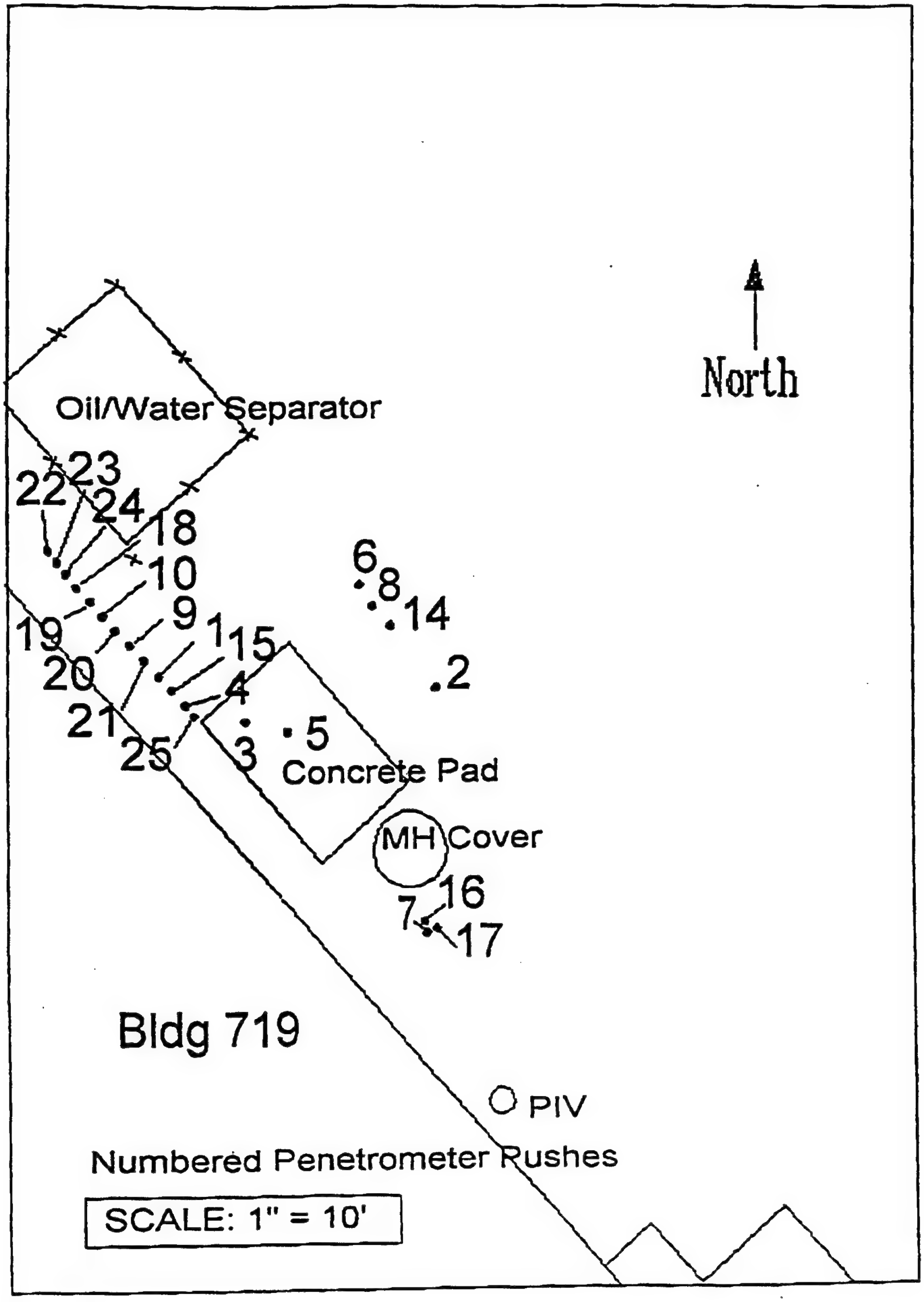

Fig. 10. Map showing locations of holes near Bldg 719. Fiber optic infrared pushes were made in Holes 9,10 and 14. Additional pushes not shown on map were made in Hole 11 (airport taxiway) and Holes 12 and 13 (golf course). [Map courtesy of Dr. W. Davis, WES.]

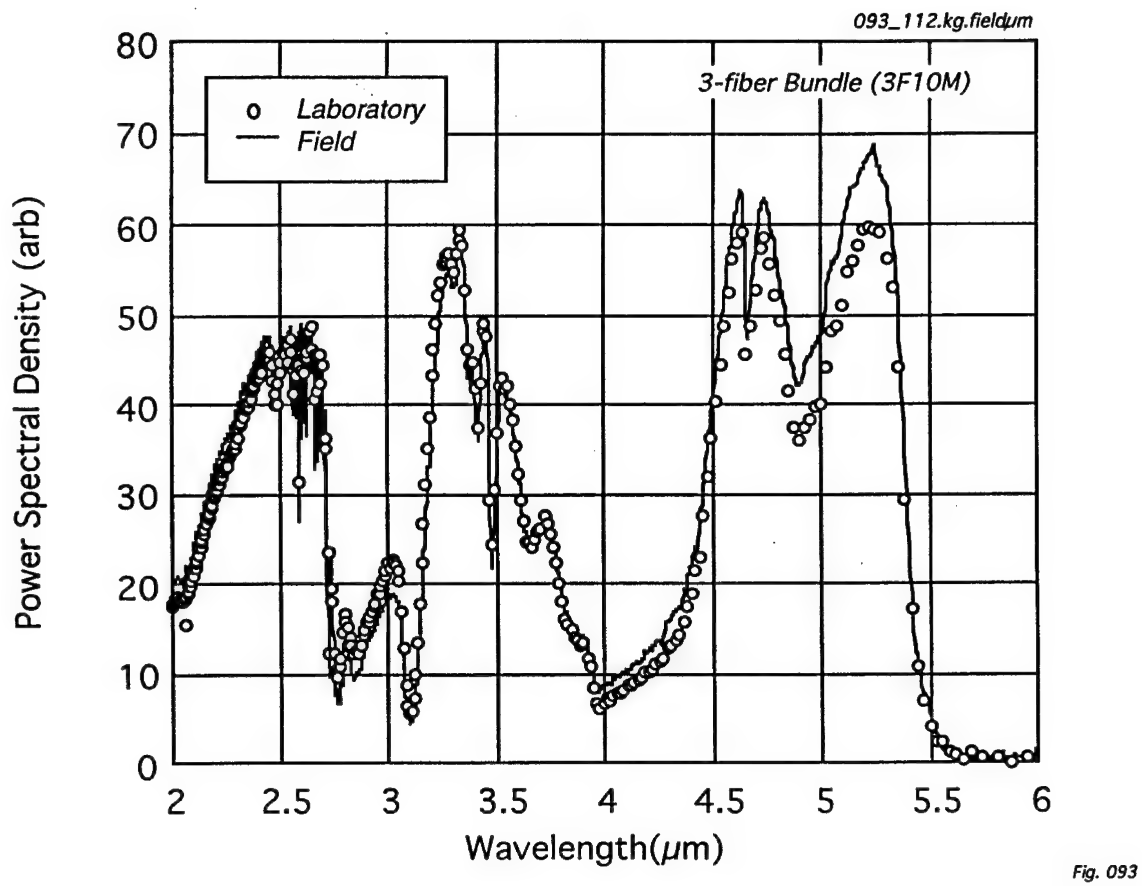

Fig. 11. *Comparison of optical throughput of cabled chalcogenide fiber in the laboratory and in the field after approximately 1-1/2 days of use in the SCAPS truck.*

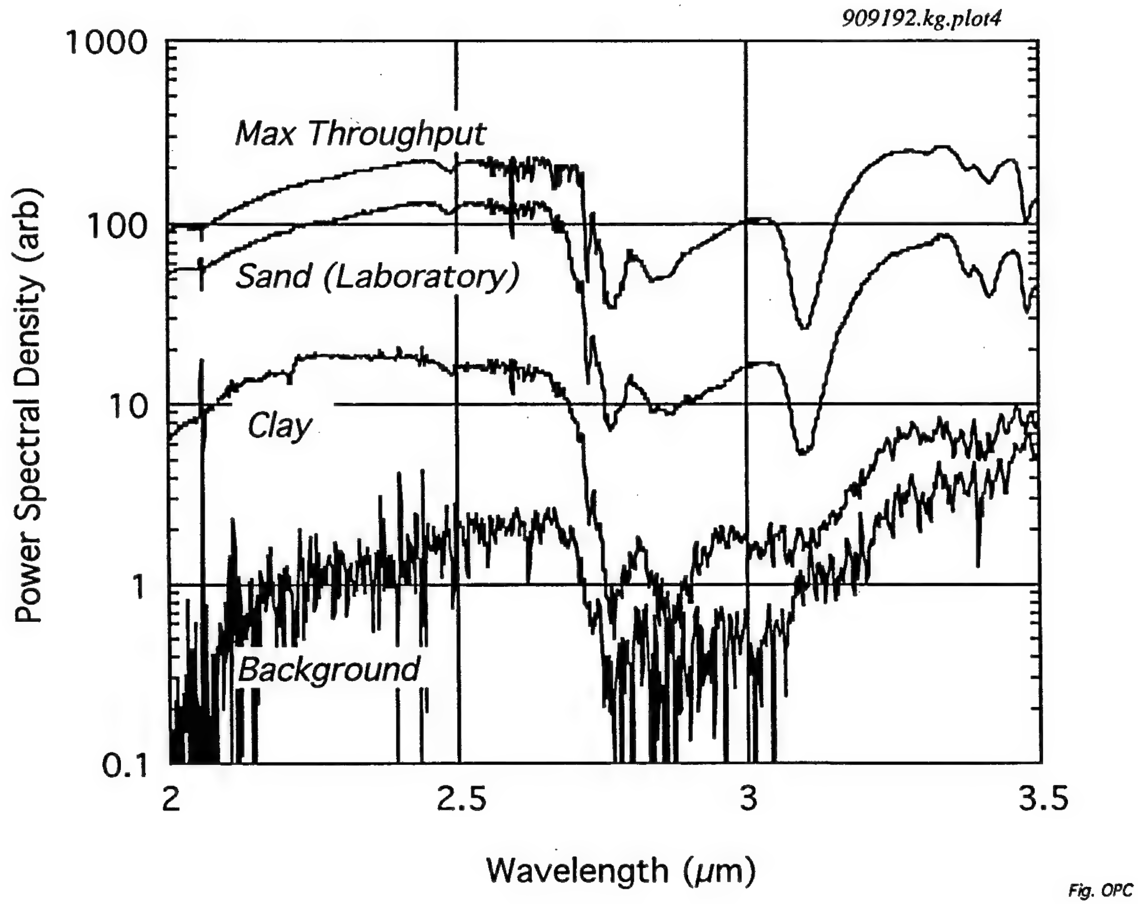

Fig. 12. Comparison of the raw optical power levels observed i) in the field with the gold reflector (Max throughput), ii) in the laboratory with a dry sand in a sample cell, iii) in the field in clay at Dover AFB (Filename DOV063), and iv) with the cable disconnected from the FTIR top show the background radiation spectrum. Spectra shown here are not normalized.

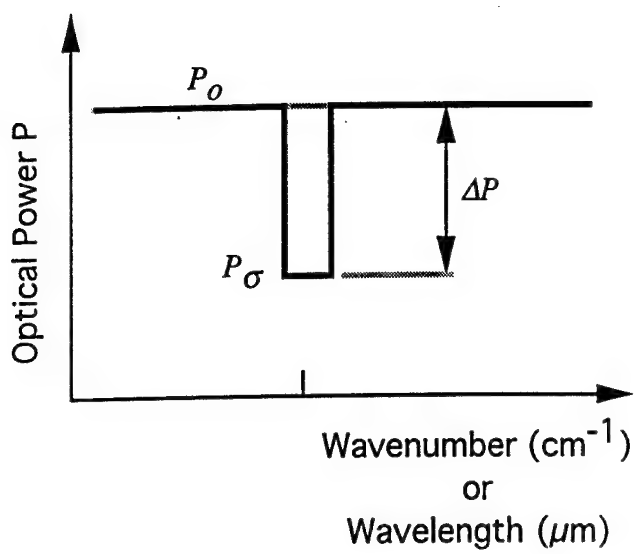

Fig. 13. Simplified model of absorption band depth $\Delta P/P_o$.

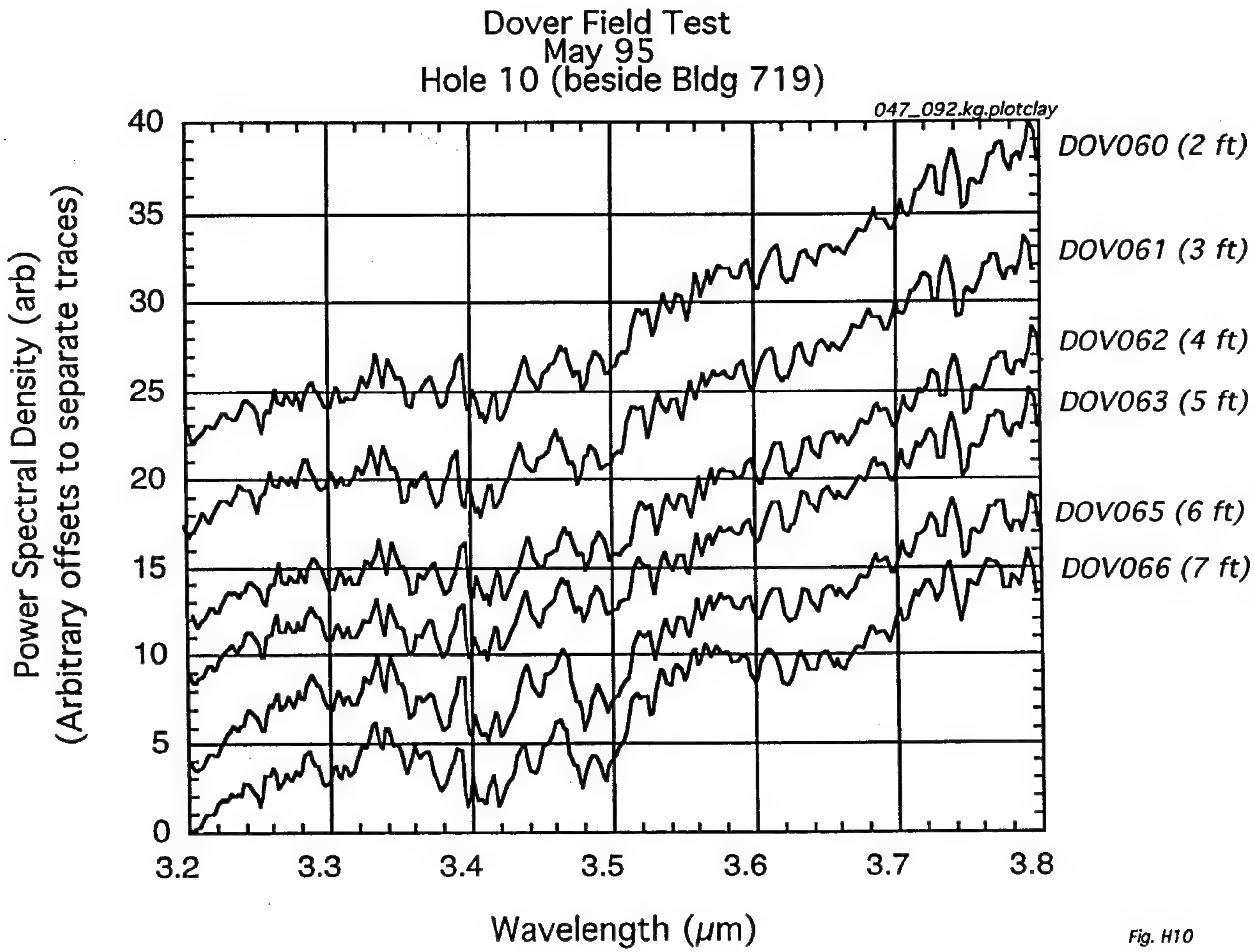

***Fig. 14**. Raw infrared power spectra at various depths in Hole 10 in the wavelength region of the C-H stretch absorption.*

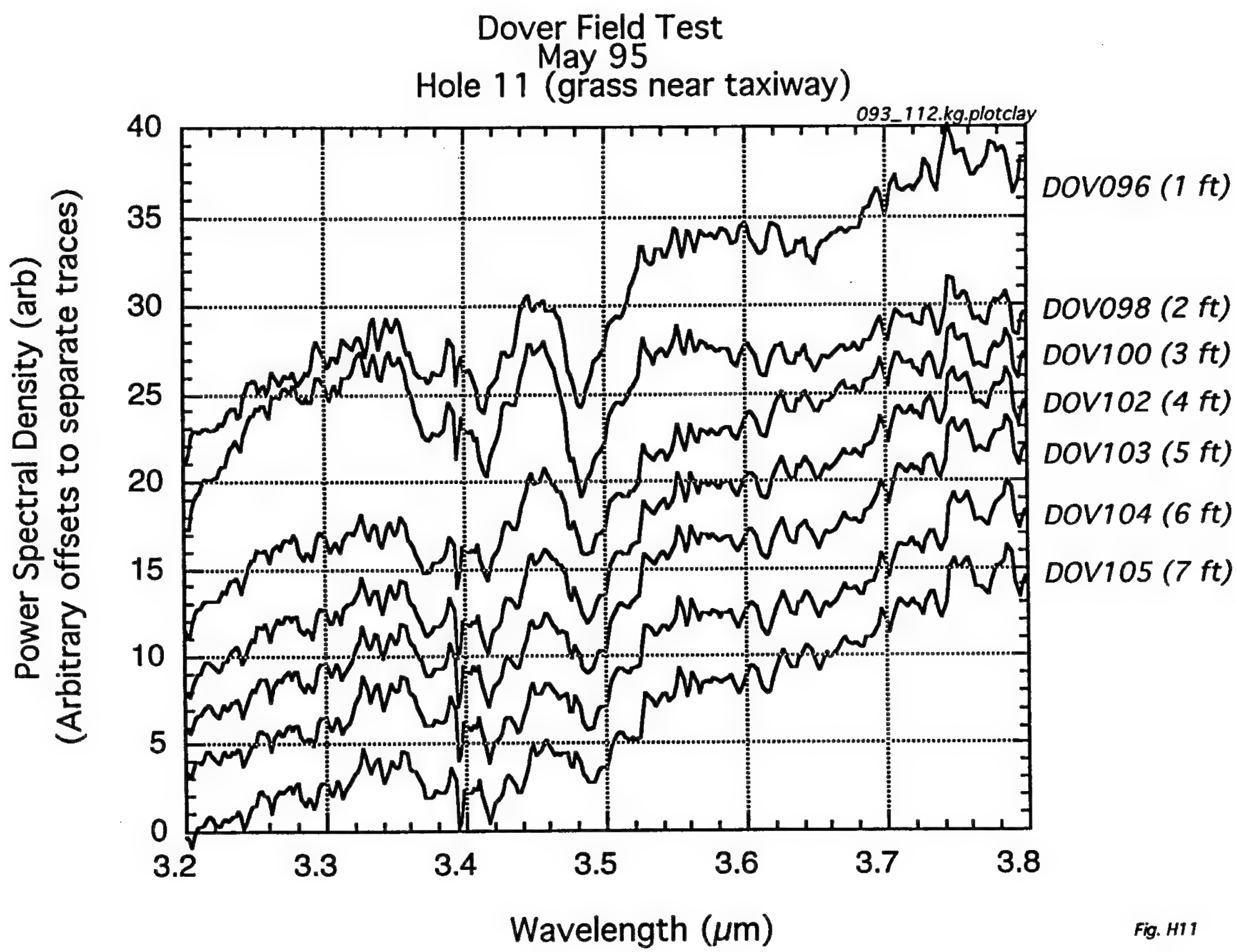

Fig. 15. *Raw infrared power spectra at various depths in Hole 11 in the wavelength region of the C-H stretch absorption.*

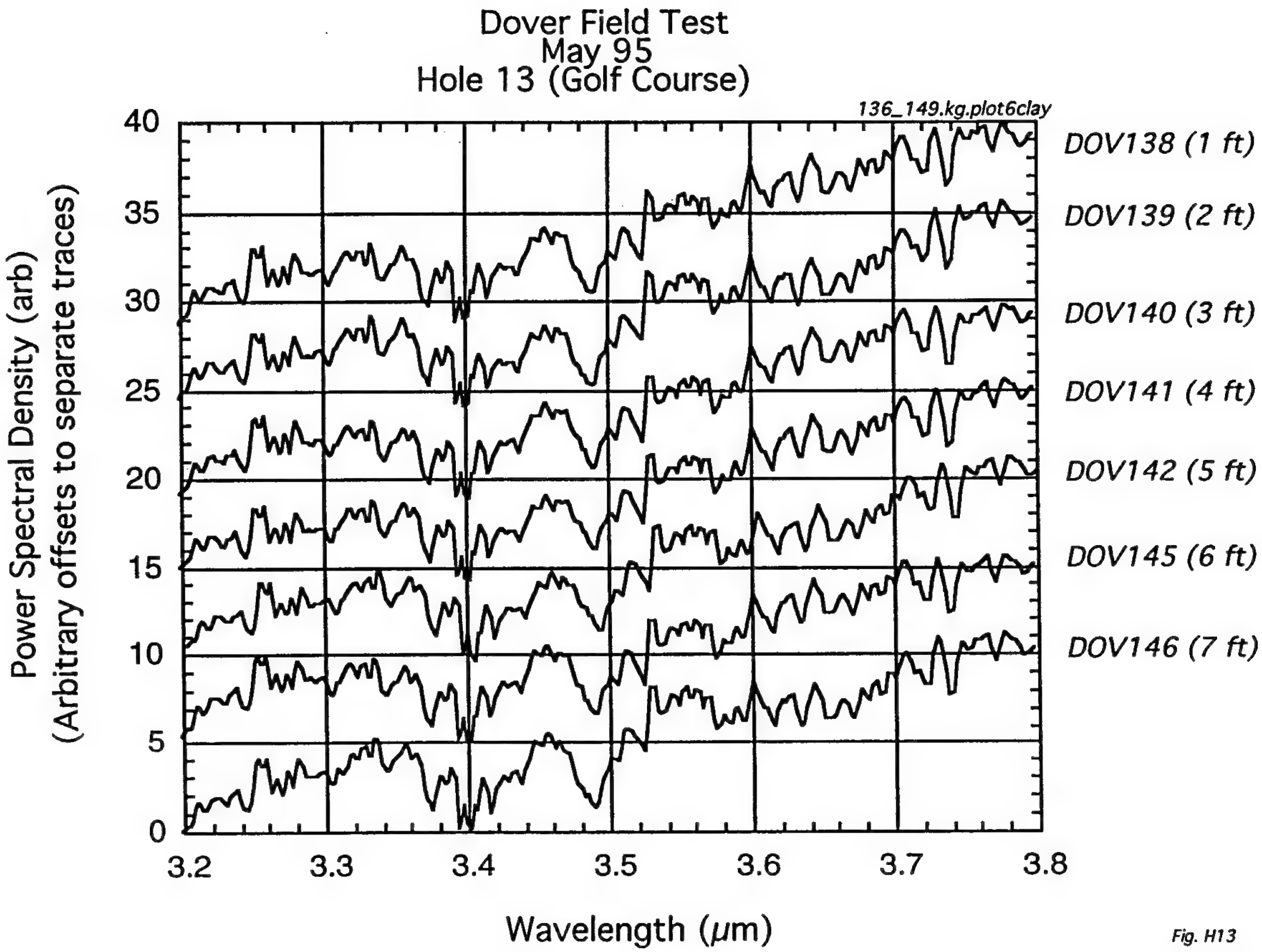

Fig. 16. *Raw infrared power spectra at various depths in Hole 13 in the wavelength region of the C-H stretch absorption.*

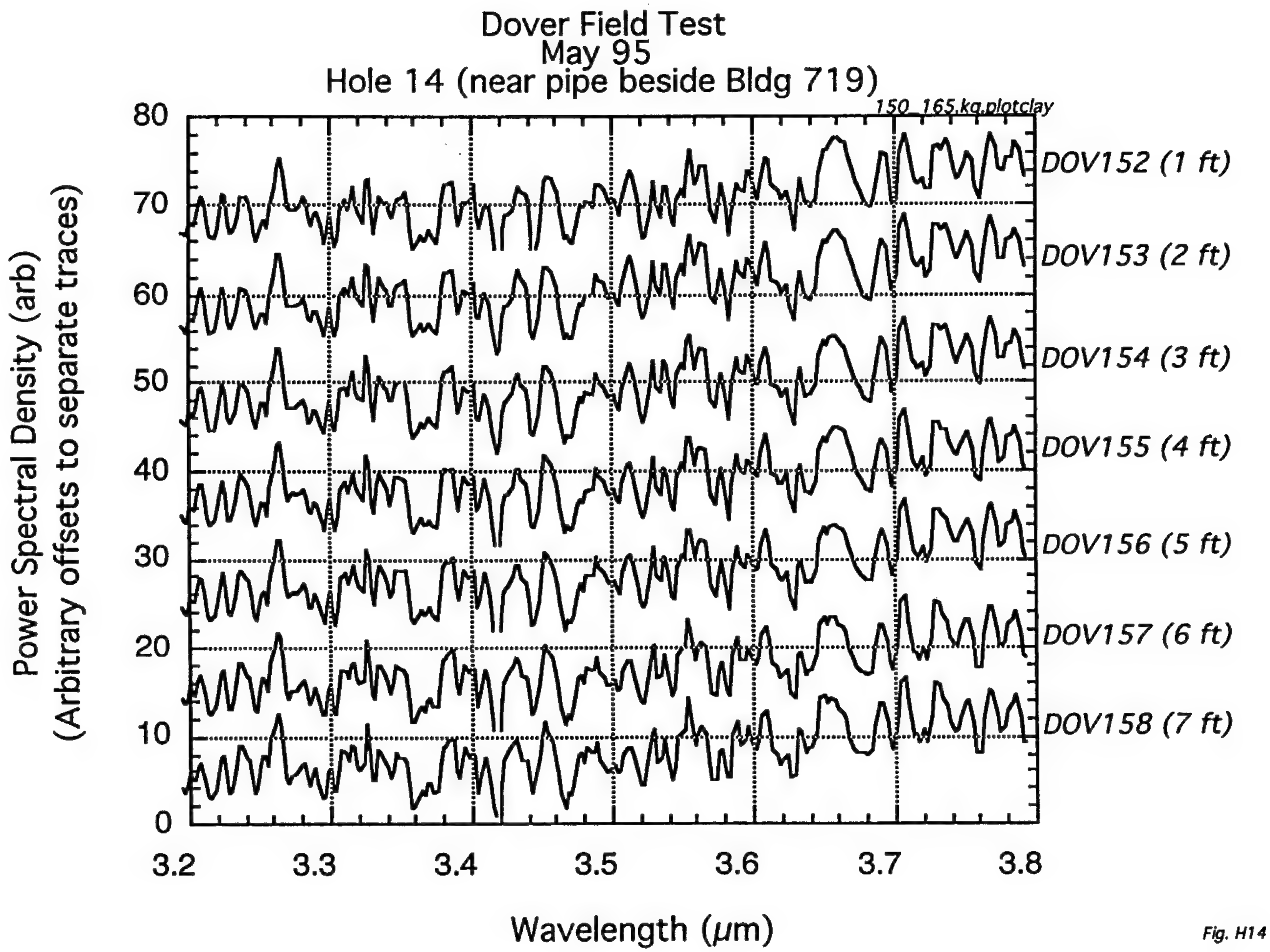

Fig. 17. *Raw infrared power spectra at various depths in Hole 14 in the wavelength region of the C-H stretch absorption.*

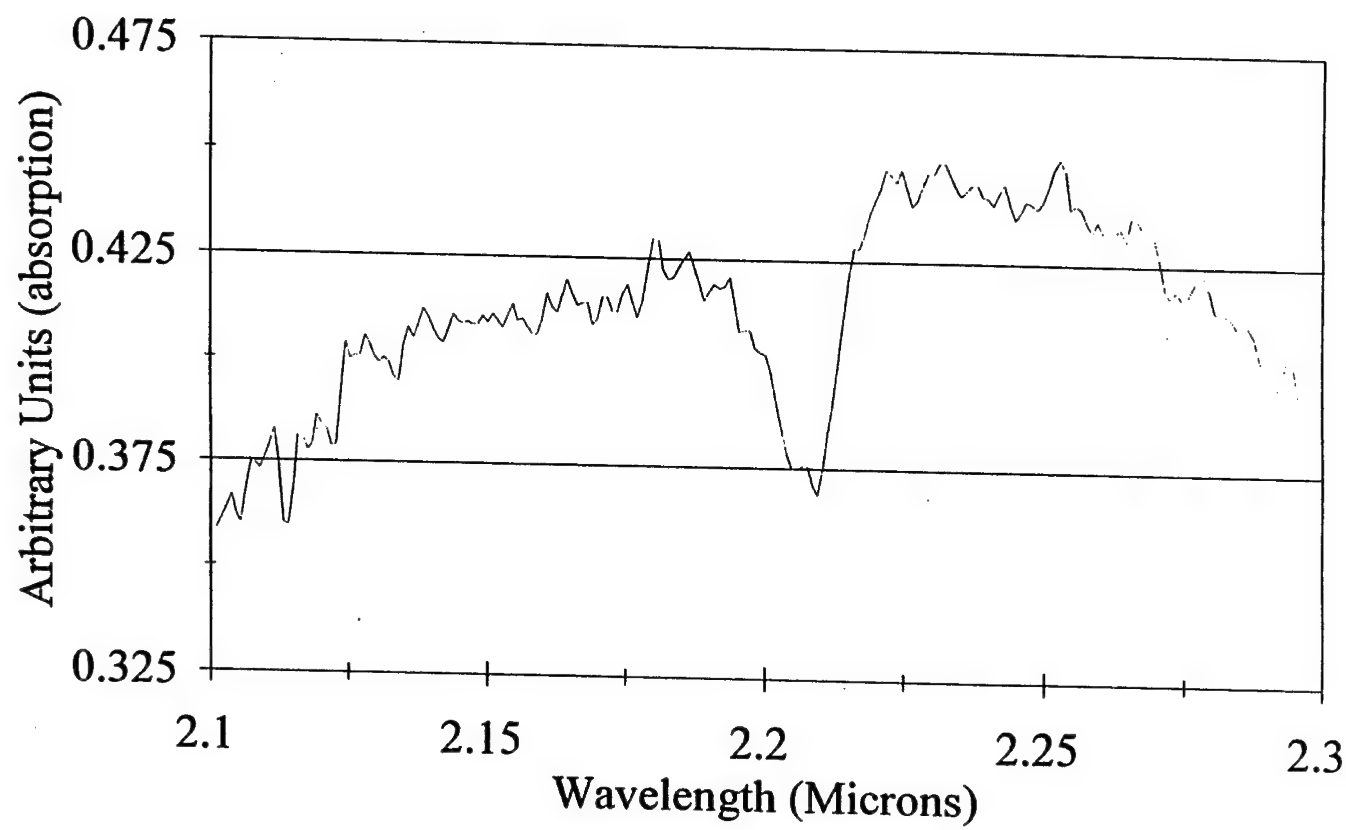

Fig. 18. Observation of the absorption doublet due to kaolinite obtained in Hole 10 at 5 ft depth. Spectrum shown has been normailized by the instrument transfer function.

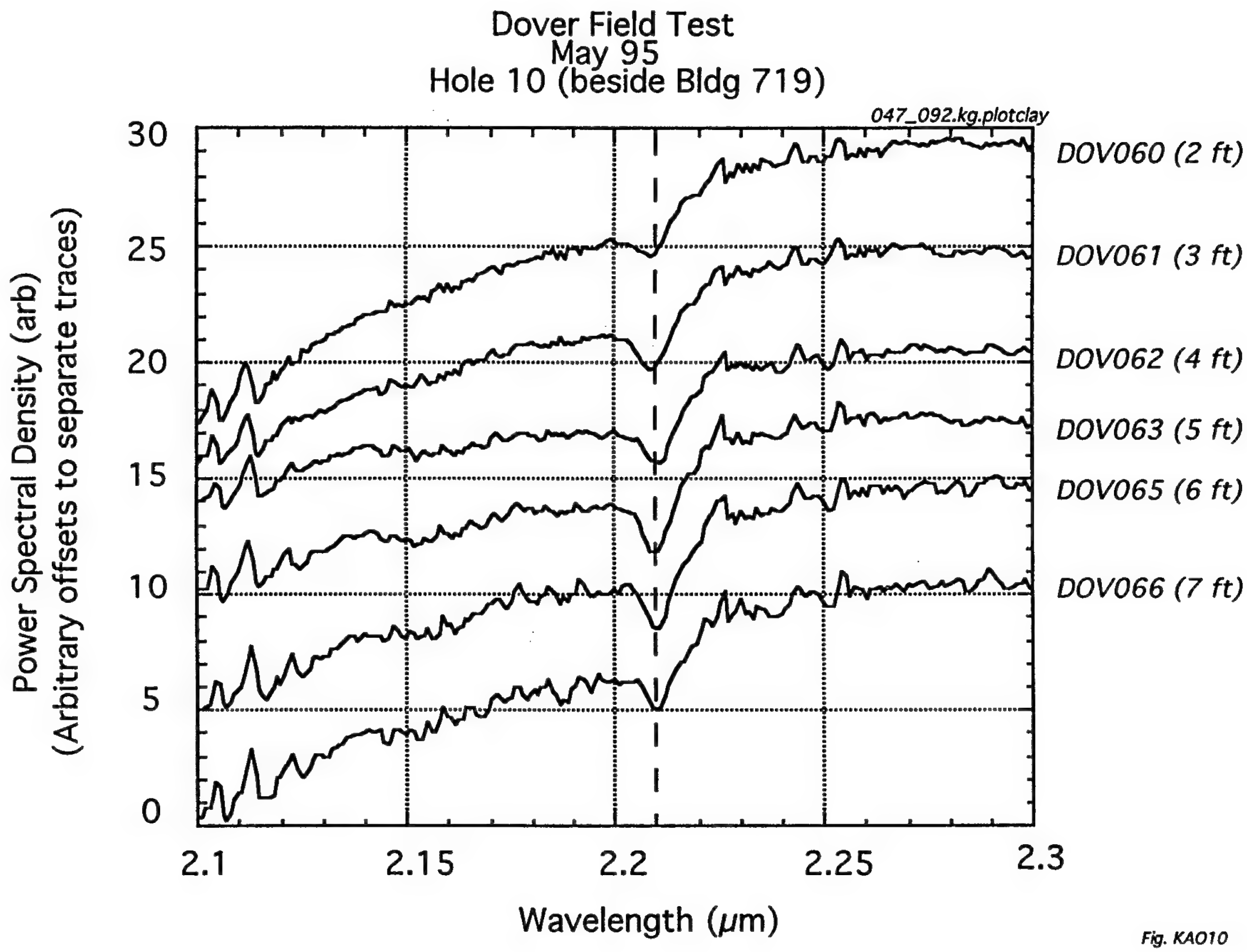

Fig. 19. Raw infrared power spectra at various depths in Hole 10 in the wavelength region of the Kaolinite absorption feature at 2.21 μm (dashed line).

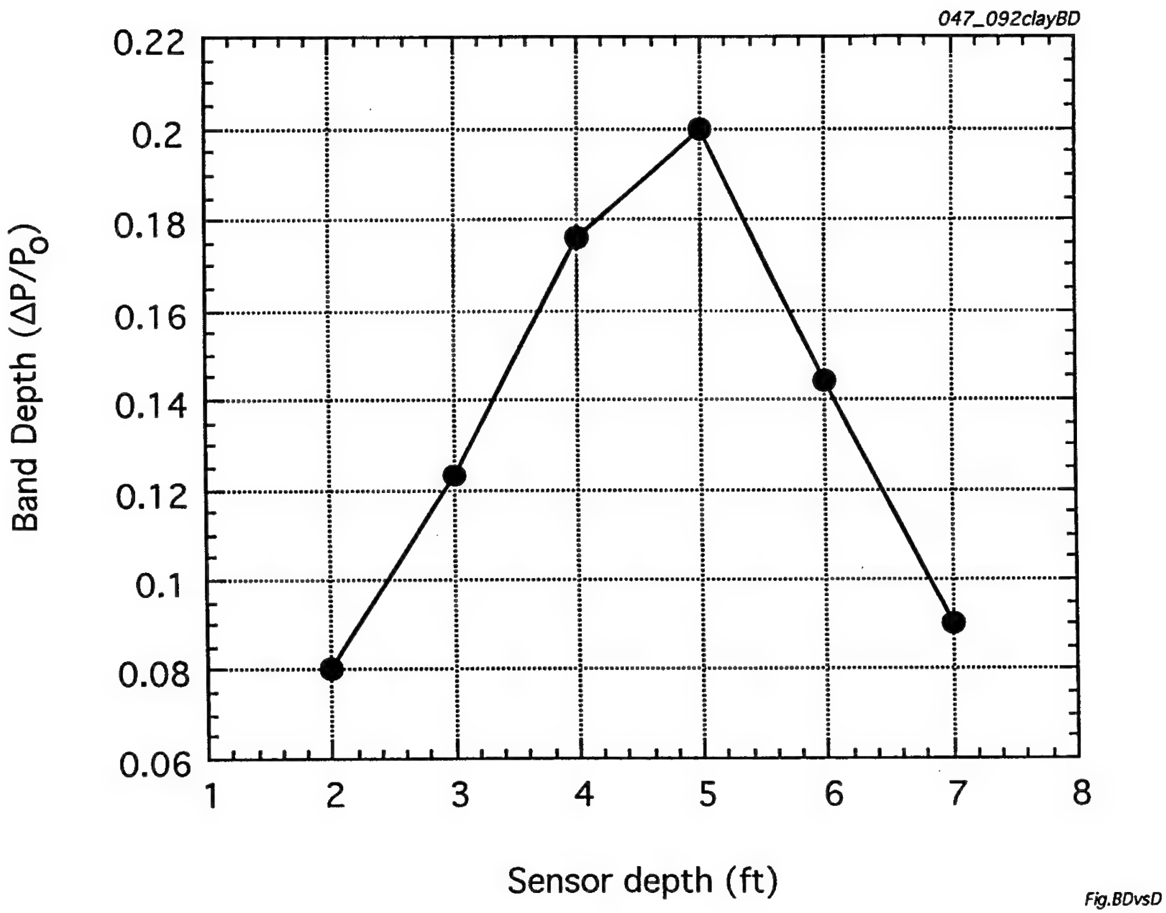

Fig. 20. *Variation in absorption band depth (after normalization) versus sensor depth for the push in Hole 10 (Fig. 19).*

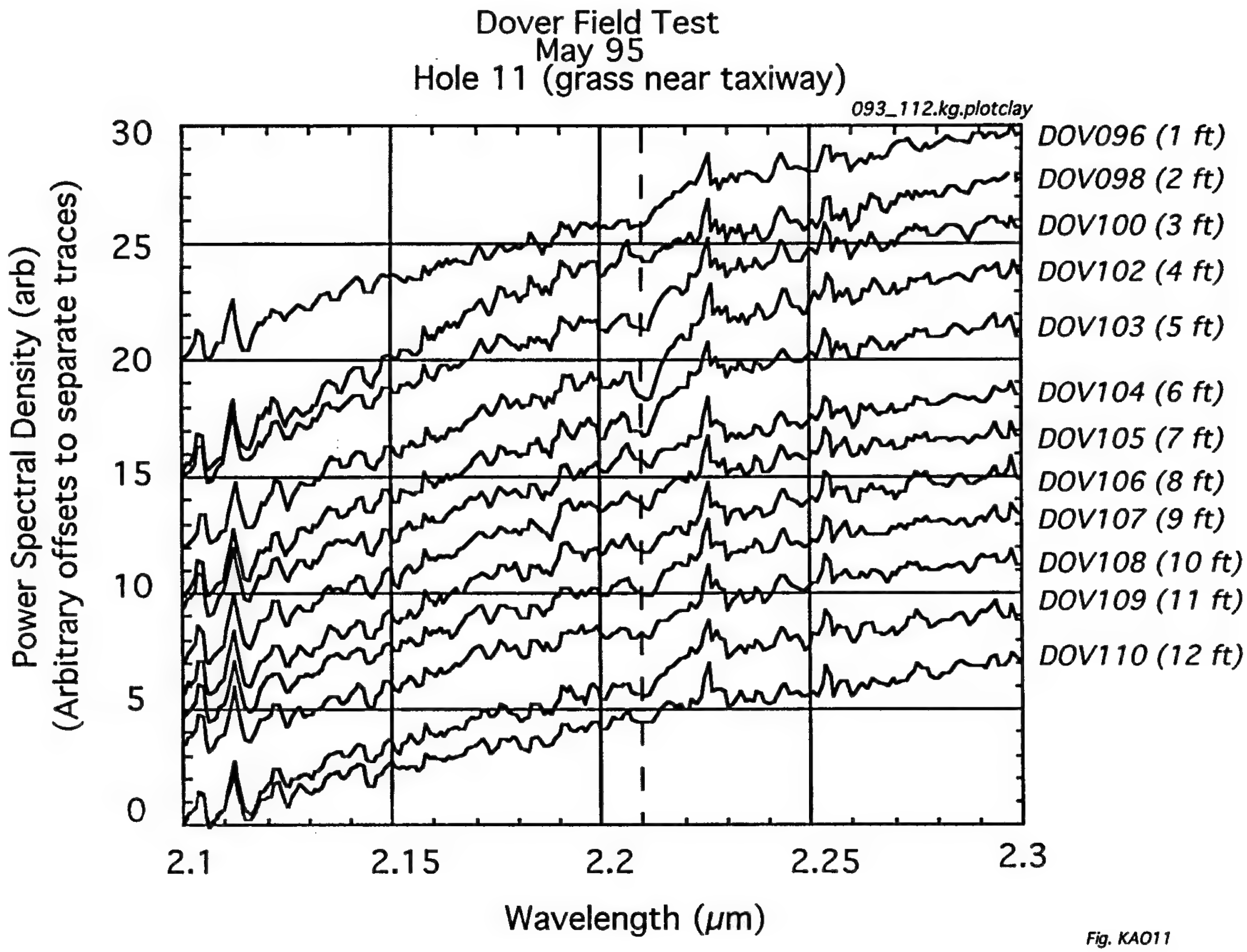

Fig. 21. *Raw infrared power spectra at various depths in Hole 13 in the wavelength region of the Kaolinite absorption feature at 2.21 μm (dashed line).*

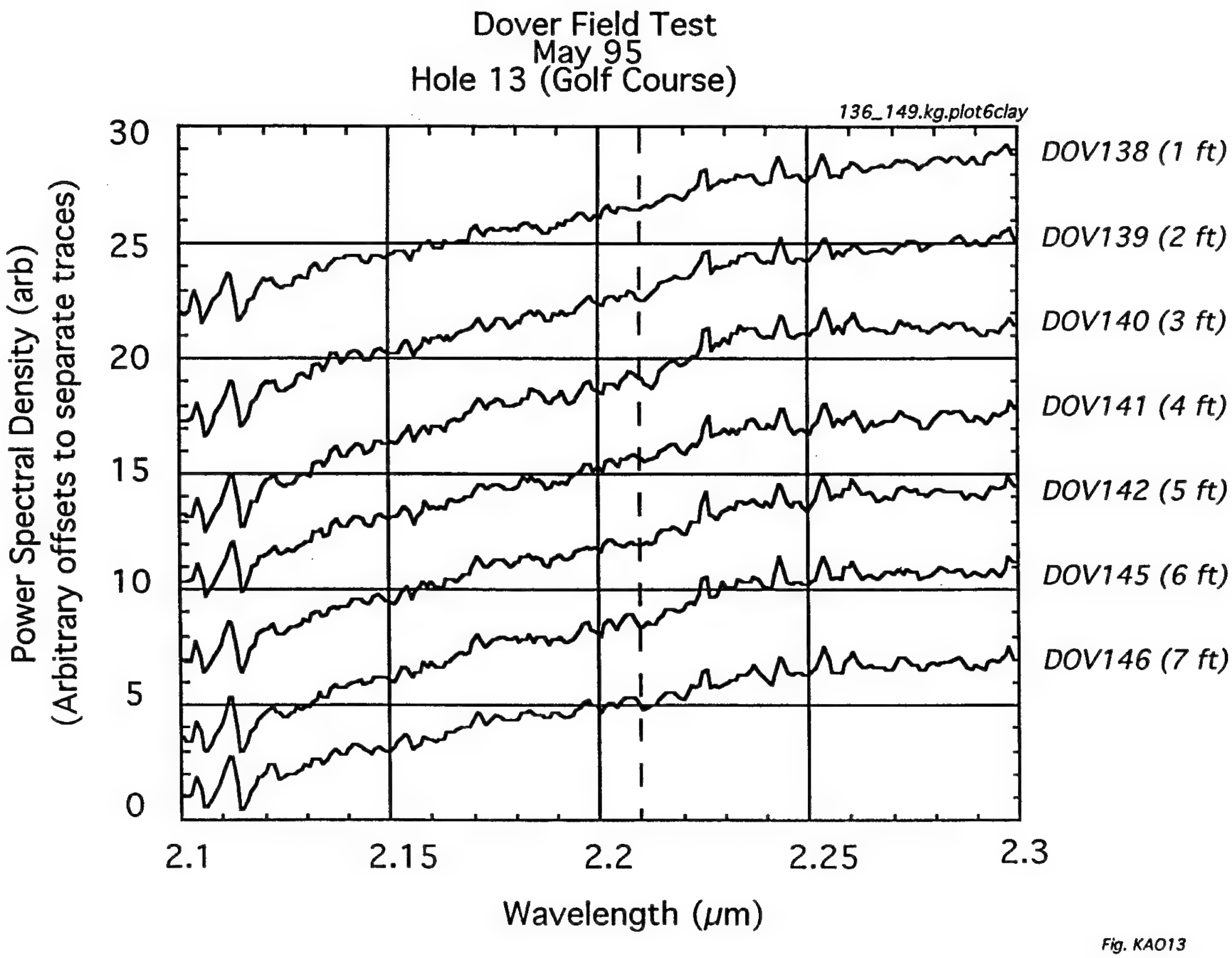

Fig. 22. *Raw infrared power spectra at various depths in Hole 13 in the wavelength region of the Kaolinite absorption feature at 2.21 μm (dashed line).*

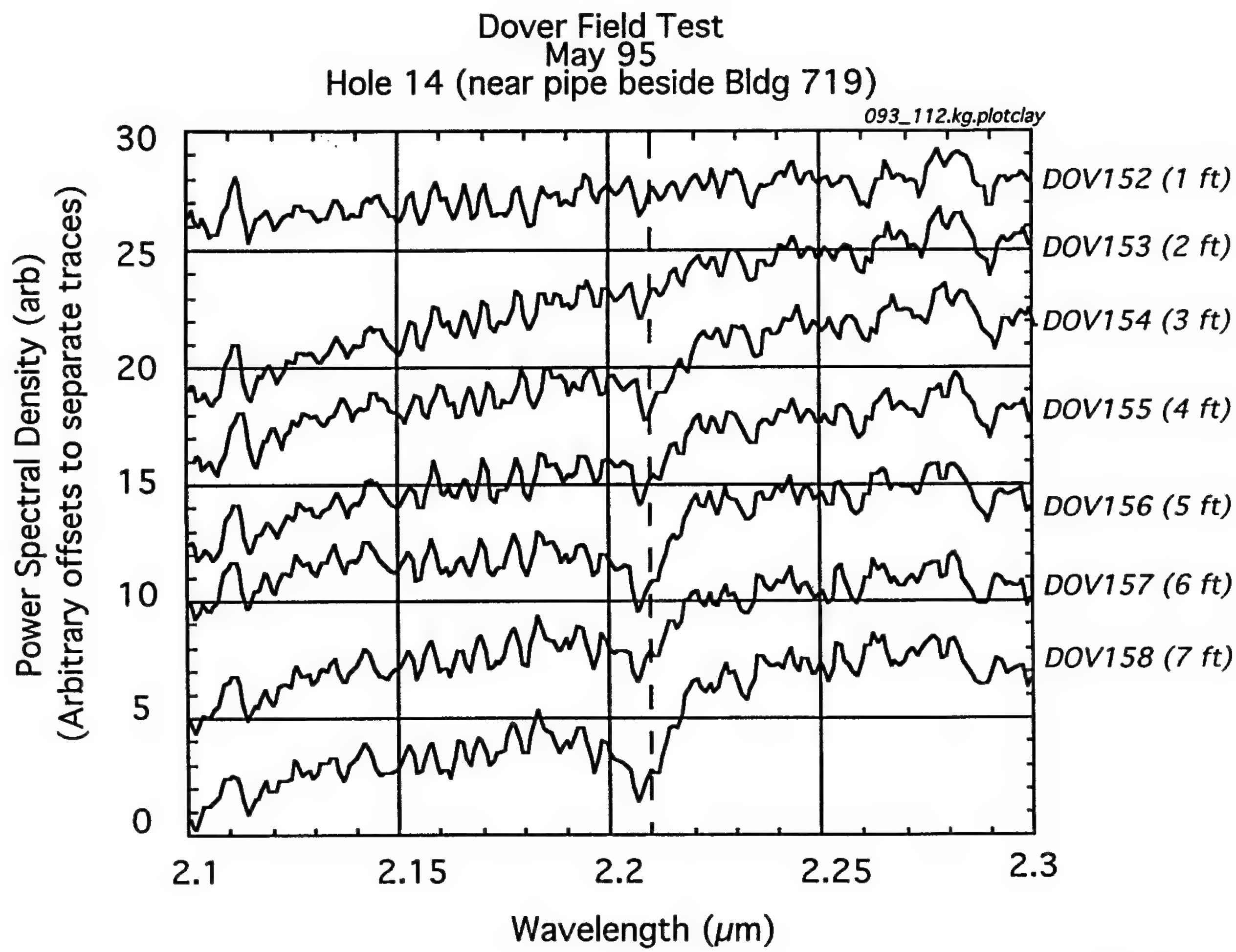

Fig. KA014

Fig. 23. Raw infrared power spectra at various depths in Hole 14 in the wavelength region of the Kaolinite absorption feature at 2.21 μm (dashed line).

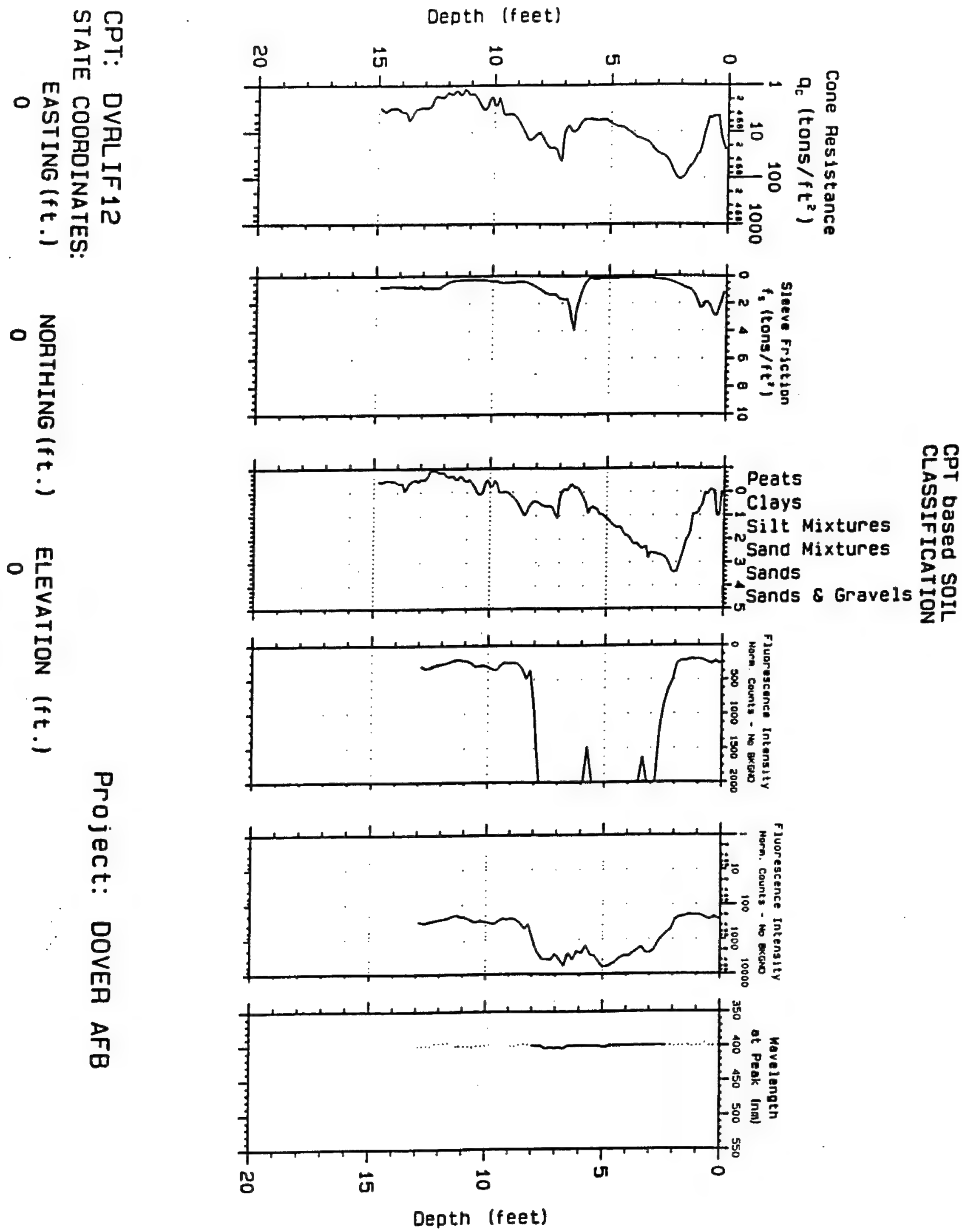

Fig. 24. Data obtained with the SCAPS soil classification and laser-induced fluorescence (LIF) system taken near Holes 12 and 13.

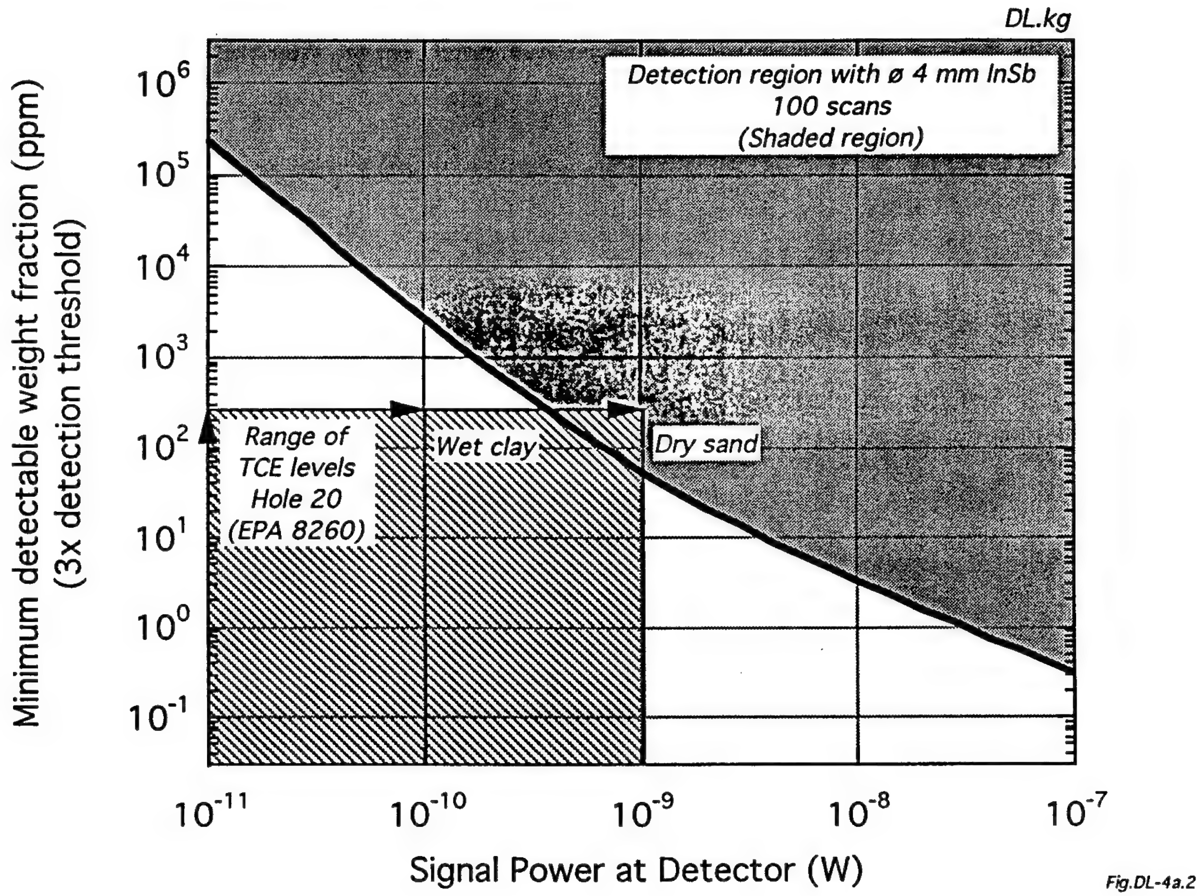

Fig.25. Expected mid-IR minimum detectable hydrocarbon level (ppm) as a function of optical signal power at the detector for the system used in the field test (solid curve). Minimum detectable weight fraction corresponds to a signal equal to three times the detection threshold (unity signal-to-noise). Shaded region in upper right shows detection region and shaded box in lower left corresponds to available signal power for the TCE concentration levels for Hole 20 determined by laboratory analysis (App. B).

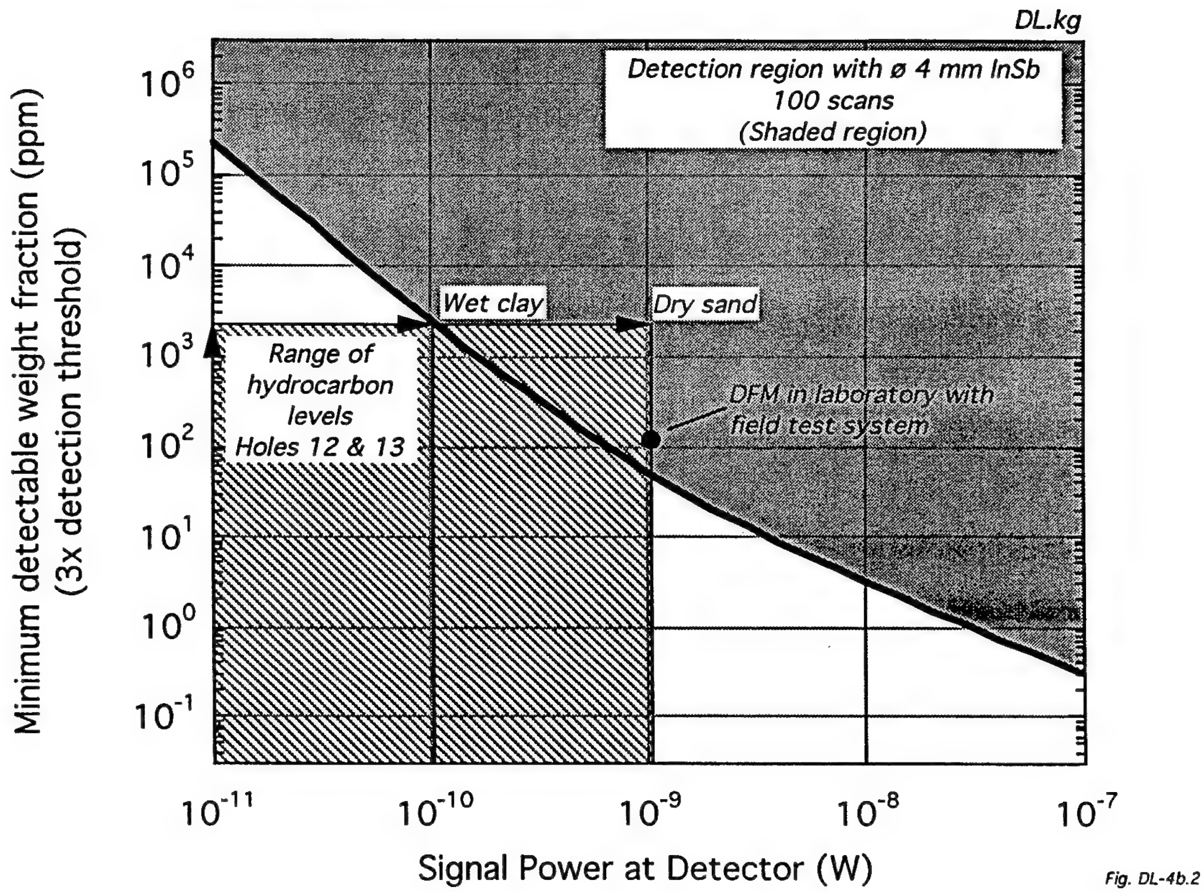

Fig. 26. Expected minimum detectable hydrocarbon level (ppm) as a function of optical signal power at the detector for the system used in the field test (solid curve). Minimum detectable weight fraction corresponds to a signal equal to three times the detection threshold (unity signal-to-noise). Shaded region in upper right shows detection region and shaded box in lower left corresponds to available signal power for the heavy hydrocarbon concentration levels near Holes 12 &13 determined by laboratory analysis (App. C). In wet clay, the available signal power was close to the detection limit.

Appendix A

Tabulation of Data Filenames
and
Measurement Parameters

Date: 8 May 95
Hole(WES): 9
Cable: 1F20M

Filename	Gain	A/D (%)	# Scans	Depth (ft)	Comments
DOV001	32	20	200	out	Gold reflector; Kepco 3.5A @ 5.2V
DOV002	32	30	200	1.0	
DOV003	32	31	200	2.0	
DOV004	32	31	200	3.0	
DOV005	32	31	200	4.0	
DOV006	32	30.8	200	5.0	
DOV007	32	31	200	6.0	
DOV008	32	31	200	6.5	
DOV009	32	31.2	200	7.0	
DOV010	32	31.2	200	7.5	
DOV011	32	31.2	200	8.0	
DOV012	32	31.2	200	8.5	
DOV013	32	31.5	200	9.0	
DOV014	32	31.5	200	9.5	
DOV015	32	31.6	200	10.0	Carl thinks water table ~ 10 ft
DOV016	32	31.8	200	10.5	
DOV017	32	31.8	200	11.0	
DOV018	32	31.1	200	12.0	
DOV019	32	31.4	200	13.0	
DOV020	32	31.8	200	14.0	
DOV021	32	31.6	200	15.0	
DOV022	32	31.8	200	18.0	
DOV023	32	32.4	200	15.0	Adjust Kepco to 3.6A @ 5.5V
DOV024	32	32.5	400	10.0	
DOV025	32	32.6	400	8.0	
DOV026	32	32.9	400	7.0	

DOV027	32	33.6	400	6.0	
DOV028	32	33.6	400	3.0	
DOV029	32	32.8	400	out	empty window
DOV030	32	43.8	400	out	gold reflector
DOV031	32	36.1	400	na	cable disconnected

Date: 8 May 95
Hole(WES): 9
Cable: 3F10M

Filename	Gain	A/D (%)	# Scans	Depth (ft)	Comments
DOV032	16	48	200	na	gold reflector
DOV033	64	45.3	400	12.0	
DOV034	64	44.1	400	11.0	
DOV035	64	44.6	400	10.0	
DOV036	64	45.0	400	9.0	
DOV037	64	44.5	400	8.0	
DOV038	64	44.7	400	7.0	
DOV039	64	44.2	400	6.0	
DOV040	64	44.1	400	5.0	
DOV041	64	44.5	400	4.0	
DOV042	64	44.7	400	3.0	
DOV043	64	46	400	2.0	
DOV044	16	49	400	out	gold reflector
DOV045	64	40.9	400	out	window empty
DOV046	64	37.7	400	na	cable disconnected

Date: 9 May 95
Hole(WES): 10
Cable: 3F10M

Filename	Gain	A/D (%)	# Scans	Depth (ft)	Comments
DOV047	16	45	10	out	gold reflector; Kepco @ 5.0V
DOV048	16	"	10	out	"
DOV049	16	"	10	out	"
DOV050	16	"	10	out	"
DOV051	16	"	100	out	"
DOV052	16	"	100	out	"
DOV053	16	"	100	out	"
DOV054	16	"	100	out	"
DOV055	16	"	1000	uot	"
DOV056	16	"	1000	out	"
DOV057	16	"	1000	out	"
DOV058	16	"	1000	out	"
DOV059	64	46.2	200	out	window empty
DOV060	64	52	200	2.0	
DOV061	64	49.5	200	3.0	
DOV062	64	46	200	4.0	
DOV063	64	46.3	200	5.0	
DOV064	64	48	200	6.0	
DOV065	64	42.7	200	6.5	
DOV066	64	45	200	7.0	
DOV067	64	42	200	7.5	
DOV068	64	44	200	8.0	
DOV069	64	41.7	200	9.0	
DOV070	64	41.3	200	10.0	topped off LN2
DOV071	64	41	100	10.0	
DOV072	64	41	200	10.0	

DOV073	64	41	200	10.0	
DOV074	64	41	200	10.0	
DOV075	64	nr	200	10.0	Jeff thinks clay below 5 ft
DOV076	64	40.6	400	8.25	
DOV077	64	nr	20	5.2	20 scans every 30 seconds for files 077 - 086
DOV078	64	nr	20	5.2	
DOV079	64	nr	20	5.2	
DOV080	64	nr	20	5.2	
DOV081	64	nr	20	5.2	
DOV082	64	nr	20	5.2	
DOV083	64	nr	20	5.2	
DOV084	64	nr	20	5.2	
DOV085	64	nr	20	5.2	
DOV086	64	nr	20	5.2	
DOV087	64	38.6	200	4.0	
DOV088	64	40	200	3.0	
DOV089	64	42	200	2.0	
DOV090	64	37.6	200	out	window empty
DOV091	8	22	200	out	gold reflector
DOV092	64	nr	200	out	cable disconnected

Date: 9 May 95
Hole(WES): 11
Cable: 3F10M

Filename	Gain	A/D (%)	# Scans	Depth (ft)	Comments
DOV093	16	51	200	out	gold reference
DOV094	16	51	200	out	gold reference
DOV095	64	42	200	out	window empty
DOV096	64	51.4	200	1.0	
DOV097	64	39	200	1.5	
DOV098	64	59	200	2.0	
DOV099	64	nr	200	2.5	
DOV100	64	50	200	3.0	
DOV101	64	46	200	3.5	
DOV102	64	49	200	4.0	
DOV103	64	48	200	5.0	
DOV104	64	43	200	6.0	
DOV105	64	44	200	7.0	
DOV106	64	46	200	8.0	
DOV107	64	44	200	9.0	
DOV108	64	46	200	10	
DOV109	64	46	200	11	
DOV110	64	44	200	11.9	
DOV111	16	59	200	out	gold reference
DOV112	64	39	200	out	window empty
DOV113					
DOV114					

Date: 9 May 95
Hole(WES): 12
Cable: 3F10M

Filename	Gain	A/D (%)	# Scans	Depth (ft)	Comments
DOV113	16	53	200	out	gold ref
DOV114	na	na	na	na	removed LN2 purge line. Discovered penetrometer tube was bent !!!

Date: 10 May 95
Hole(WES): 13
Cable: 3F10M

Filename	Gain	A/D (%)	# Scans	Depth (ft)	Comments
DOV115	16	44	200	out	gold reference; Kepco 3.5A @ 5.0V
DOV116	64	nr	200	out	gold reference
DOV117	64	29	200	out	empty window
DOV118	64	31	200	1	
DOV119	64	32	200	2	
DOV120	64	31	200	3	
DOV121	64	32	200	4	
DOV122	64	32	200	4	
DOV123	64	33	200	5	
DOV124	64	33	200	5	
DOV125	64	33	200	5	
DOV126	64	33	200	5	
DOV127	64	33	200	5	
DOV128	64	32	200	6	Noticeable drop in overall signal
DOV129	64	34	200	7	
DOV130	64	33	200	8	

DOV131	64	31	200	out	empty window
DOV132	8	21	200	out	gold reference
DOV133	16	42	200	out	gold reference
DOV134	64	31	200	out	cable disconnected
DOV135	64	31	200	out	cable disconnected
DOV136	16	38	200	out	gold reference
DOV137	64	32	200	out	empty window
DOV138	64	34	200	1.0	
DOV139	64	35	200	2.0	
DOV140	64	36	200	3.0	
DOV141	64	34	200	4.0	
DOV142	64	35	200	5.0	
DOV143	64	35	200	5.0	
DOV144	64	35	200	5.0	
DOV145	64	34	200	6.0	
DOV146	64	34	200	7.0	
DOV147	64	31	200	out	empty window
DOV148	16	42	200	out	gold reference
DOV149	64	31	200	out	cable disconnected

Date: 11 May 95
Hole(WES): 14
Cable: 3F10M

Filename	Gain	A/D (%)	# Scans	Depth (ft)	Comments
DOV150	16	38	200	out	gold reference
DOV151	64	23	200	out	window empty
DOV152	64	24	200	1	
DOV153	64	28	200	2	
DOV154	64	27	200	3	
DOV155	64	27	200	4	
DOV156	64	27	200	5	
DOV157	64	28	200	6	
DOV158	64	29	200	7	
DOV159	64	31	200	8	
DOV160	64	28	200	out	window empty
DOV161	64	28	200	out	window empty
DOV162	16	38	200	out	gold ref
DOV163	16	38	200	out	gold ref
DOV164	64	30	200	out	cable disconnected
DOV165	64	29	200	out	cable disconnected

Appendix B.

Laboratory Analytical[1] Results
of
Soil Samples[2] taken in Holes 20, 24 & 25

[1] Samples analyzed for VOC's by EPA method 8260
[2] Results courtesy of Dr. W. Davis, WES

Soil Samples @ Building 719 Dover AFB, May 1995

Method of Hewett, JAOAC, 1994, Vol. 77, 458-463

Sample	Depth ft, BGS	11DClEta (mg/kg)	c-DClEte (mg/kg)	111TCA (mg/kg)	TCE (mg/kg)	1122TClA (mg/kg)	ClBen (mg/kg)	Benzene (mg/kg)	Toluene (mg/kg)	T-Xylene (mg/kg)	EtBen (mg/kg)
20-1	4	<5.0	<5.0	4.6	<5.0	NA	<5.0	<5.0	<5.0	<5.0	<5.0
20-2	5	<5.0	<5.0	<5.0	<5.0	NA	<5.0	<5.0	<5.0	<5.0	<5.0
20-3	6	<5.0	<5.0	1.3	<5.0	NA	<5.0	<5.0	<5.0	1.2	0.31
20-4	8	<5.0	16	230	<5.0	NA	<5.0	<5.0	1.6	26	8
20-5	9	<5.0	160	660	<5.0	NA	<5.0	<5.0	<5.0	52	15
20-6	10	<5.0	51	370	5.1	NA	<5.0	<5.0	2.2	43	9.8
20-7	11	<5.0	100	410	290	NA	<5.0	<5.0	<5.0	39	9

NA indicates sample not analyzed for this chemcial

William M. Davis, 601 634 3785

Soil Samples @ Building 719 Dover AFB, May 1995

Method of Hewett, JAOAC, 1994, Vol. 77, 458-463

Sample	Depth ft, BGS	11DClEta (mg/kg)	c-DClEte (mg/kg)	111TCA (mg/kg)	TCE (mg/kg)	1122TClA (mg/kg)	ClBen (mg/kg)	Benzene (mg/kg)	Toluene (mg/kg)	T-Xylene (mg/kg)	EtBen (mg/kg)
24-01	5	<0.5	<0.5	1.49	<0.5	<0.5	<0.5	<0.5	<0.5	3.65	<0.5
24-02	5.5	<0.5	<0.5	5.47	<0.5	<0.5	<0.5	<0.5	<0.5	5.33	<0.5
24-03	6	<0.5	<0.5	3.67	<0.5	<0.5	<0.5	<0.5	<0.5	0.94	<0.5
24-04	6.5	0.90	2.33	86.92	<0.5	0.90	<0.5	<0.5	<0.5	10.75	5.56
24-05	7	2.86	2.86	75.98	<0.5	0.69	<0.5	<0.5	<0.5	8.99	4.33
24-06	7.5	<0.5	1.68	55.79	<0.5	1.16	<0.5	<0.5	<0.5	13.68	6.53
24-07	8	1.38	9.87	138.16	1.84	1.12	<0.5	<0.5	1.05	13.16	6.58
24-08	8.5	1.48	12.04	148.15	1.85	0.93	<0.5	<0.5	1.85	13.89	7.50
24-09	9	<0.5	4.37	54.71	<0.5	<0.5	<0.5	<0.5	<0.5	6.15	3.07
25-01	5	<0.5	<0.5	<0.5	<0.5	0.66	<0.5	<0.5	<0.5	<0.5	<0.5
25-02	5.5	<0.5	<0.5	<0.5	<0.5	<0.5	0.76	0.83	0.78	<0.5	<0.5
25-03	6	1.09	<0.5	2.55	<0.5	0.58	0.67	<0.5	<0.5	<0.5	<0.5
25-04	6.5	<0.5	<0.5	4.21	<0.5	1.89	<0.5	<0.5	<0.5	<0.5	<0.5
25-05	7	2.04	10.75	107.53	4.62	0.89	<0.5	<0.5	<0.5	0.96	<0.5
25-06	7.5	1.32	7.94	66.14	2.84	0.58	<0.5	<0.5	<0.5	0.63	<0.5
25-07	8	<0.5	<0.5	4.32	<0.5	<0.5	<0.5	<0.5	<0.5	<0.5	<0.5
25-08	8.5	1.60	16.01	112.99	4.90	0.76	<0.5	<0.5	<0.5	1.22	<0.5
25-09	9	1.68	17.60	120.00	5.20	0.80	<0.5	<0.5	<0.5	1.52	1.52
25-10	10	2.29	32.35	168.46	1.01	0.74	<0.5	<0.5	1.01	4.92	2.70
25-11	11	1.67	30.21	122.11	1.67	<0.5	<0.5	<0.5	1.41	3.73	1.67

Soil Samples @ Building 719 Dover AFB, May 1995

EPA Method 8260

Soil	Depth ft, BGS	11DClEta (mg/kg)	c-DClEte (mg/kg)	111TCA (mg/kg)	TCE (mg/kg)	1122TClA (mg/kg)	ClBen (mg/kg)	Benzene (mg/kg)	Toluene (mg/kg)	T-Xylene (mg/kg)	EtBen (mg/kg)
24-01	5	<6	<6	<6	<6	<6	<6	<6	<6	4.5	<6
24-02	5.5	<6	<6	<6	<6	<6	<6	<6	<6	5.1	<6
24-03	6	<5.6	<5.6	1.50	<5.6	<5.6	<5.6	<5.6	<5.6	1.7	<5.6
24-04	6.5	<5.6	<5.6	12.00	<5.6	<5.6	<5.6	<5.6	<5.6	3.4	1.60
24-05	7	<5.4	<5.4	7.40	<5.4	<5.4	<5.4	<5.4	<5.4	4.8	2.30
24-06	7.5	<5.5	<5.5	8.20	<5.5	<5.5	<5.5	<5.5	<5.5	5.2	2.50
24-07	8	<5.6	<5.6	22.00	<5.6	<5.6	<5.6	<5.6	<5.6	9.7	4.70
24-08	8.5	<5.6	<5.6	22.00	<5.6	<5.6	<5.6	<5.6	<5.6	7.9	4.70
24-09	9	<5.5	<5.5	22.00	<5.5	<5.5	<5.5	<5.5	<5.5	7.4	3.70
25-01	5	<5.9	<5.9	<5.9	<5.9	<5.9	<5.9	<5.9	<5.9	<5.9	<5.9
25-02	5.5	<.058	<.058	<.058	<.058	<.058	<.058	<.058	<.058	<.058	<.058
25-03	6	<5.5	<5.5	<5.5	<5.5	<5.5	<5.5	<5.5	<5.5	<5.5	<5.5
25-04	6.5	<5.6	1.30	40.00	1.60	<5.6	<5.6	<5.6	<5.6	1.1	0.63
25-05	7	<5.5	1.90	29.00	1.40	<5.5	<5.5	<5.5	<5.5	0.74	0.56
25-06	7.5	<5.7	1.30	26.00	1.30	<5.7	<5.7	<5.7	<5.7	0.95	0.52
25-07	8	<5.5	<5.5	10.00	<5.5	<5.5	<5.5	<5.5	<5.5	<5.5	<5.5
25-08	8.5	<5.5	<5.5	6.60	0.55	<5.5	<5.5	<5.5	<5.5	0.74	<5.5
25-09	9	<5.5	4.40	44.00	2.10	<5.5	<5.5	<5.5	<5.5	1.7	0.79
25-10	10	<5.7	0.96	10.00	<5.7	<5.7	<5.7	<5.7	<5.7	1.2	<5.7
25-11	11	<5.9	<5.9	15.00	<5.9	<5.9	<5.9	<5.9	<5.9	2.1	0.92

Appendix C

Laboratory Analytical Results
of
Soil Samples taken near Holes 12 & 13.

Gascoyne Laboratories, Inc.

Baltimore, MD 21224-6697

(410) 633-1800
(800) GAS-COYN
FAX NO.
(410) 633-5443

REPORT OF ANALYSIS

Report No.	95-06-177	Report Date:	June 29, 1995
Report To:	Naval Research Laboratory	Page:	1 of 4
Sample I.D.	Submitted Soil:		

	Semi-volatile Petroleum Hydrocarbons	Detection Limits	Date Test Completed
GC-2 ft, Sample 1	200	20	06/15/95
GC-2 ft, Sample 2	140	20	06/15/95
GC-2 ft, Sample 3	180	20	06/15/95
GC-3 ft, Sample 1	2200	20	06/17/95
GC-3 ft, Sample 2	1900	20	06/17/95
GC-2 ft, Sample 3	2400	20	06/17/95
GC-4 ft, Sample 1	ND	20	06/16/95
GC-4 ft, Sample 2	ND	20	06/17/95
GC-4 ft, Sample 3	ND	20	06/17/95
GC-5 ft, Sample 1	600	20	06/17/95
GC-5 ft, Sample 2	560	20	06/17/95
GC-5 ft, Sample 3	410	20	06/17/95

Notes:
(1) Results expressed as mg/kg (ppm) on an as received basis.
(2) Reported as diesel fuel oil, defined as C_{10} to C_{23} hydrocarbons.
(3) Analyses were performed according to the methods outlined in the California Leaking Underground Fuel Tank Manual, May 1988, pages 60-72
(4) Analyst(s): MLS
(5) Sampling date unknown.
(6) Samples tumbled for one hour prior to extraction.

Thomas A. McVicker
QA/QC Officer

Gascoyne Laboratories, Inc.

Baltimore, MD 21224-6697

(410) 633-1800
(800) GAS-COYN
FAX NO.
(410) 633-5443

REPORT OF ANALYSIS

Report No. 95-06-177 Report Date: June 29, 1995

Report To: Naval Research Laboratory Page: 2 of 4

Sample I.D. Submitted Soil:

	Semi-volatile Petroleum Hydrocarbons	Detection Limits	Date Test Completed
GC-7 ft, Sample 1	1500	20	06/17/95
GC-7 ft, Sample 2	1100	20	06/17/95
GC-7 ft, Sample 3	1500	20	06/17/95
Sample A, Sample 1	160	20	06/17/95
Sample A, Sample 2	140	20	06/17/95
Sample A, Sample 3	140	20	06/17/95
Sample B, Sample 1	270	20	06/15/95
Sample B, Sample 2	270	20	06/15/95
Sample B, Sample 3	240	20	06/16/95
Sample C, Sample 1	580	20	06/15/95
Sample C, Sample 2	620	20	06/16/95
Sample C, Sample 3	610	20	06/16/95

Notes:
(1) Results expressed as mg/kg (ppm) on an as received basis.
(2) Reported as diesel fuel oil, defined as C_{10} to C_{23} hydrocarbons.
(3) Analyses were performed according to the methods outlined in the California Leaking Underground Fuel Tank Manual, May 1988, pages 60-72
(4) Analyst(s): MLS
(5) Sampling date unknown.
(6) Samples tumbled for one hour prior to extraction.

Thomas A. McVicker
QA/QC Officer